



REVIEW

Tribological and Mechanical Performance of Coatings on Piston to Avoid Failure—A Review

Santosh Kumar · Manoj Kumar

Submitted: 15 April 2022/in revised form: 24 May 2022/Accepted: 6 June 2022/Published online: 23 June 2022
© ASM International 2022

Abstract Piston is the most important part in internal combustion engine. During engine operation, piston experiences stress, pressure, temperature change resulting in mechanical and thermal fatigue failure. In addition, the seizure of pistons due to their contact with the piston rings, skirt and cylinder liners is among the major problem in internal combustion engines, posing a serious threat to the efficiency of the automobiles. Hence, the aim of this review paper is to provide an overview of distinct causes of piston failures and their preventive measures. Further, the tribological and mechanical properties (hardness, elastic modulus, coefficient of friction, roughness, wear rate) of different coatings deposited by various researchers on piston/cylinder liner/piston ring are summarized. These results help the researchers in selecting an appropriate coating material composition, coating process, and parameters for a particular piston/cylinder liner/piston ring material to enhance the life of piston system. So, that any unwanted damage of piston system due to stress, pressure, fatigue, wear and friction could be minimized.

Keywords Engine piston · Piston rings · Failures · Mechanical fatigue · Tribology · Preventive measures · Coating

Introduction

The overall performance of internal combustion engine is affected by friction and wear in different engine components. The various parts of internal combustion engine include the following: cylinder, piston, crankshaft, connecting rod, cylinder head, etc. These parts are given complex shapes owing to its functional requirements which further involve comparatively complex manufacturing [1]. Deulgaonkar et al. [2] analyzed the failure data of 50 engines & 8 major parts of engine (valves, camshaft, bearing, connecting rod, cooling system, crankshaft, piston and cylinder block) using visual inspection of broken parts, water testing of engine cylinder block for internal crack and SEM/EDS analysis. Then, the number of failures detected in the 8 main engine parts is noted as depicted in Table 1.

Further, the number of failures occurred w.r.t. engine components is depicted in Fig. 1a.

Finally, the risk priority number (RPN) associated with every failure is calculated to prioritize the components for experimental analysis. The RPN is calculated by using the formula:

$$RPN = S \times O \times D$$

where, S= severity number, which is assigned based upon the severity of failure; O: number of times the particular engine part failed; D: number of times the failure was detected

Then, based upon the RPN obtained for each engine parts graph is plotted as depicted in Fig. 1b.

From Fig. 1a, number of failures in piston and cylinder block is highest and poses a serious threat to the efficiency of the automobile. In addition, among various engine parts, piston is one of the main parts which suffer major wear

S. Kumar (✉)
Department of Mechanical Engineering, Chandigarh Group of Colleges Landran, Mohali, Punjab, India
e-mail: santoshdgc@gmail.com

M. Kumar
Department of Mechanical Engineering, Chandigarh University, Gharuan, Mohali, Punjab, India

Table 1 Number of failures observed in the 8 main engine parts

Engine part	No. of time the engine part failed	No. of times the failure detected
Valves	1	4
Camshaft	1	4
Bearing	3	4
Connecting rod	3	6
Cooling system	7	3
Crankshaft	8	5
Piston	13	4
Cylinder block	14	5

losses due to friction under different speed and load conditions. However, the loss due to friction is the main reason for increasing the overall fuel consumption by 25%. These frictional losses in internal combustion engine take place at distinct engine components, including piston system, gear, cylinder and bearings. Among these engine parts, piston system is the primary contributors for friction. It is estimated that 50 to 65% frictional losses occurs in piston system. The piston ring and cylinder block share the remaining frictional losses [3]. In addition, due to the presence of poor piston ring sealing, the oil consumption increases [2]. Further, during engine operation the piston is exposed to very high gas temperature (up to 2500 °C) and pressures (8 MPa) [4]. This high operating temperature results in piston failure. As the losses due to friction are much higher in piston rings than other sliding parts so the losses owing to friction must be decreased as much as possible for enhancing fuel efficiency [5, 6]. But, in spite of many investigations on the piston, its failure is still usual phenomena. The failure of the piston and rings occurs due to many reasons. The distinct origins of piston failures are shown in Fig. 2.

However, the seizure of piston skirt is also a common problem in internal combustion engine. The piston skirt indicates axial scoring sign mainly on the thrust side. The common causes of piston skirt seizure are shown in Fig. 3.

The piston must possess high strength and heat-resistant characteristics to resist inertia forces and gas pressure. In other words, the design of engine component, especially piston, should be such that it should have less weight, friction and resistant to oxidation and corrosion at high flaming temperature [13]. In addition, the perfect sealing on the piston ring surface is also essential for mainly two reasons (a) to prevent the fuel loss occurred during the compression stroke (b) to create the pressure required for heating the fuel.

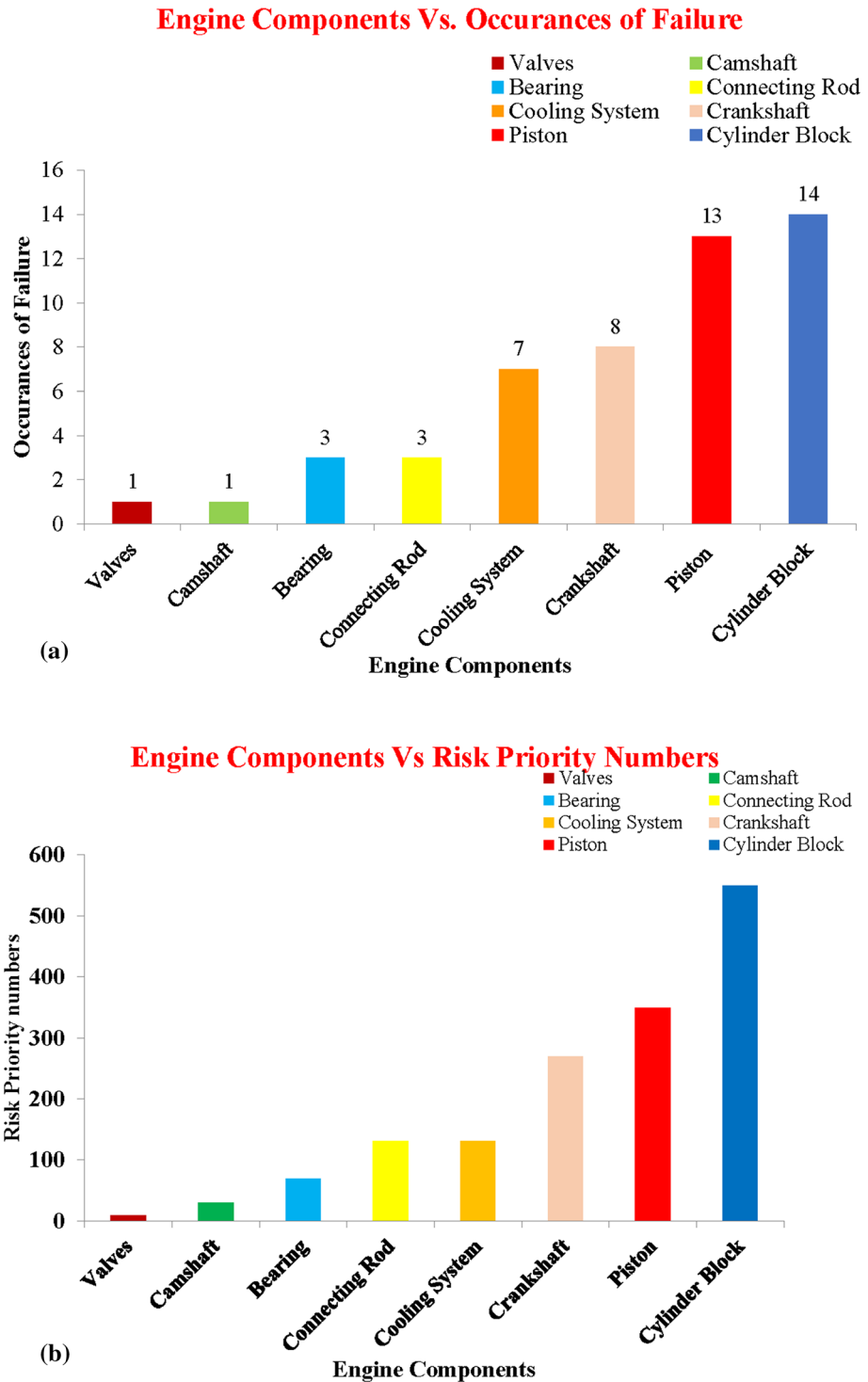
During combustion stroke, the friction between piston rings and piston will be more owing to thermal expansion. Simultaneously improper sealing of piston rings allows lubricants to enter the combustion chamber. This leads to the mixing of fuel with lubricants and results in incomplete combustion of fuel. Further, these dilutions of lubrication oil result in wear and tear of the engine parts. Hence, piston rings are utilized to wipe out excessive oil from the chamber wall and to prevent the lubricating oil from dilution [14]. So, in order to solve these problems proper sealing with low friction is requisite to enhance the overall performance of the internal combustion engine. This can be achieved by depositing the material having a low coefficient of friction using advanced coating processes. Thus, by developing an appropriate coating on piston skirts is the best way to diminish noise, friction, and scuffing. It also helps to overcome the decreasing oil viscosity and increasing the peak-cylinder-pressure in heavy-duty compression ignition engines.

Presently, various authors have used distinct advanced coatings to reduce wear, roughness, friction and improve mechanical properties of the piston. These coatings include organic coating, anodizing, electrochemical plating, vapor phase processes and hybrid coatings, etc. But coating by physical vapor deposition is gaining more attention due to its flexible characteristics, sustainability and environmentally friendly. Physical vapor deposition is a vacuum thin layer deposition technique mainly utilized for enhancing tribological and mechanical characteristics of the material [15]. This process was first used by Michael Faraday in 1838. After that this process is most widely used for high melting point and low vapor pressure materials due to its attractive properties. It is a versatile technique and involves condensation and evaporation of material. Further, with the advancement in PVD techniques, the use of thinner surface coating having better mechanical characteristics as compared to substrate material became well known among the piston ring manufacturer.

Literature Review

The thermal efficiency of internal combustion engine can be enhanced by diminishing the heat loss through the exhaust gases and improving the combustion process. This can be achieved by depositing thermal barrier coatings on the piston. This will also lead to increase the tribological performance of the piston and decrease the emission as well as specific fuel consumption. Various researchers have been applied distinct coatings by a distinct coating process to improve the wear and corrosion performance of the piston system [15].

Fig. 1 (a) Bar graph between the numbers of times the failure occurrences w.r.t. engine parts. Reprinted by permission from Elsevier: Elsevier, *Engineering Failure Analysis*, Failure analysis of diesel engine piston in transport utility vehicles, Vikas Radhakrishna Deulgaonkar,Nupoor Ingolikar,AtharvaBorkar,Sagar Ghute,Neha Awate, Copyright 2021, [2]. (b) Risk priority number w.r.t. various engine parts. Reprinted by permission from Elsevier: Elsevier, *Engineering Failure Analysis*, Failure analysis of diesel engine piston in transport utility vehicles, Vikas Radhakrishna Deulgaonkar,Nupoor Ingolikar,AtharvaBorkar,Sagar Ghute,Neha Awate, Copyright 2021, [2]



Ozkan et al. [16] deposited graphene oxide coating on piston ring by chemical vapor deposition method and decreased the resistance against corrosion of substrate steel by 7.84 mm/year to 0.16 mm/year and enhanced the corrosion protection efficiency of substrate by 97%. Further, the result of immersion tests indicates that graphene oxide

has excellent resistance against corrosion in harsh corrosive environment (1M H₂SO₄) as depicted in Fig. 4.

Further, the deposited coating enhanced the resistance against wear. Hence, the graphene oxide coating is a good candidate to resist corrosion and wear of piston rings of internal combustion engine.

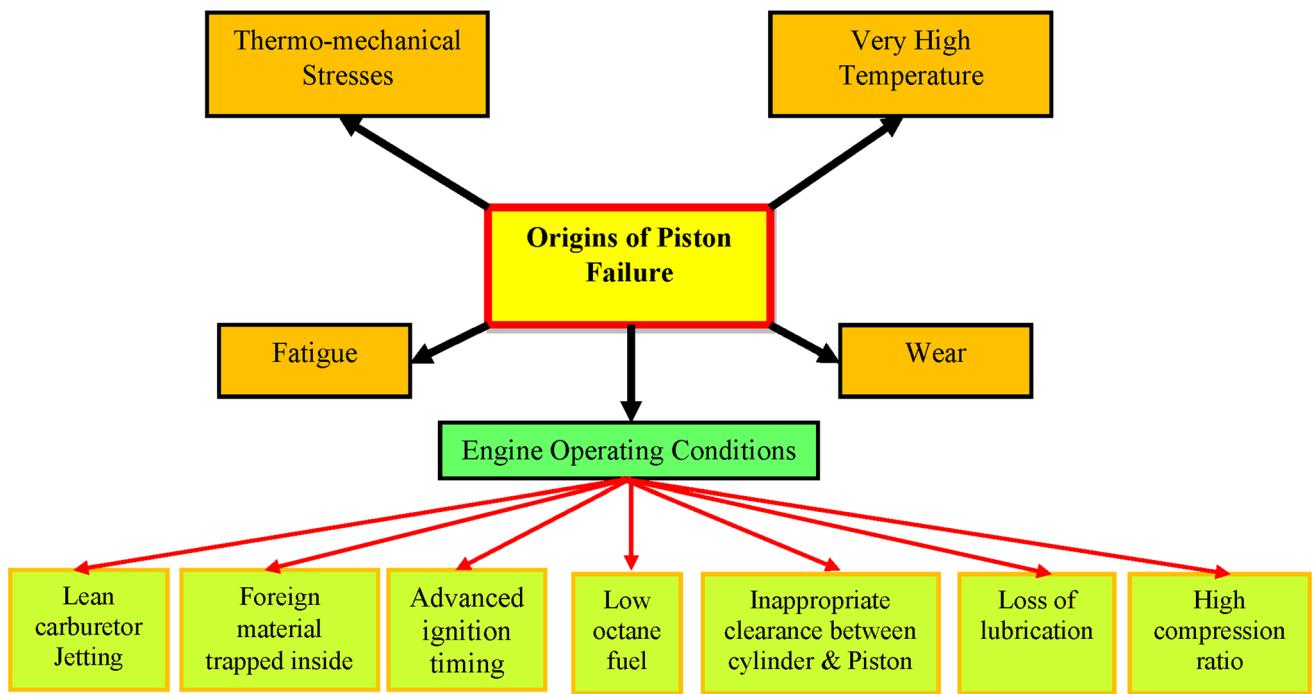


Fig. 2 Various origin of piston failure [7–10]

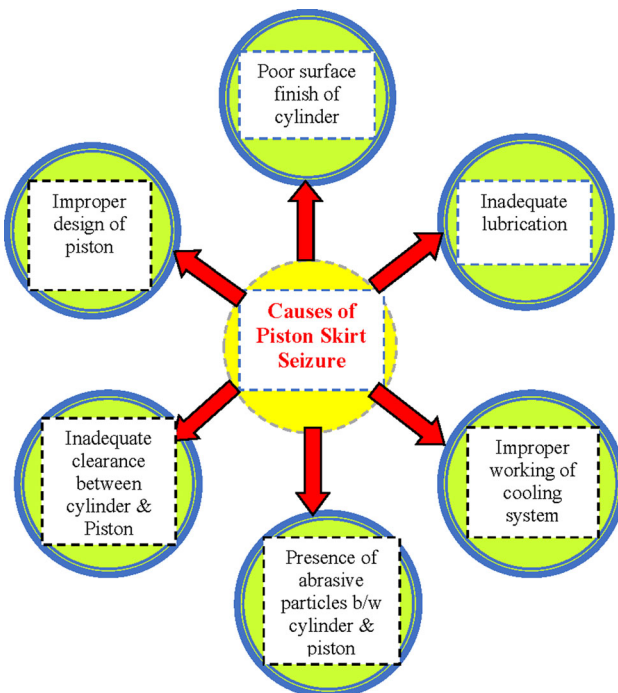


Fig. 3 Causes of internal combustion engine piston skirt seizure [11, 12]

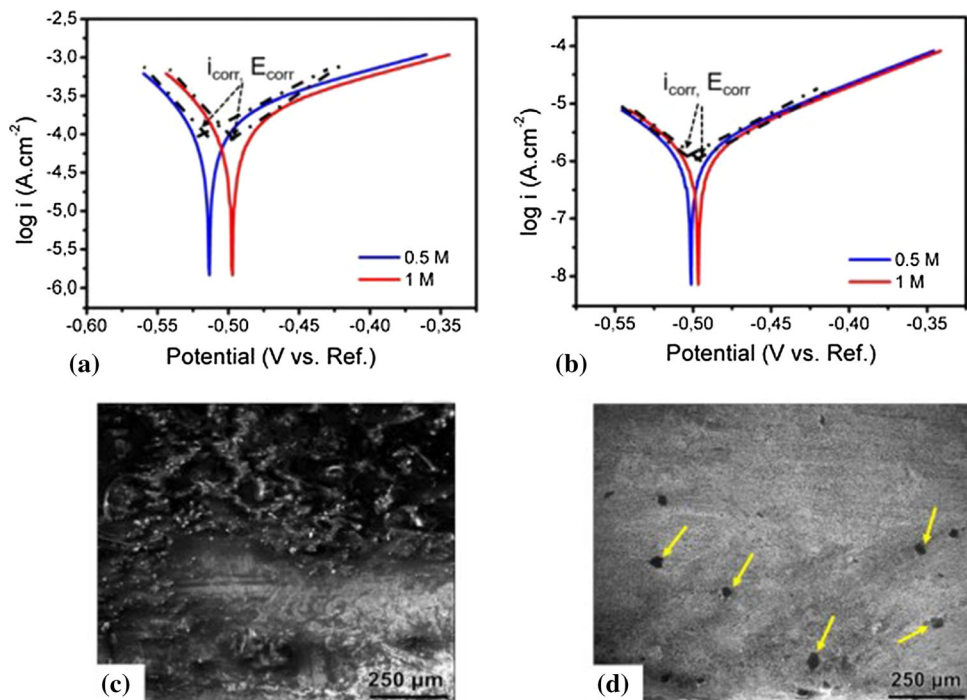
Kumar et al. [17] investigated the performance of hard diamond-like carbon (DLC) and tungsten carbide (WC) coatings on piston rings. The coatings were deposited by PVD process. Thereafter, epoxy/grapheme/base oil SN 150 composite coating was deposited on the DLC and WC

coatings. The tribological test results showed that the DLC hard and soft polymer composite dual coating over the top piston ring was observed to have the lowest wear rate ($1.69 \times 10^{-12} \text{ mm}^3/\text{Nm}$) than the wear rate of dual coatings on lower and middle rings. However, lower piston rings exhibited higher wear rate owing to delamination of deposited coating. This delamination of coating attributed to the dynamics of engine vibration and less bond strength between the coating and substrate. Thus, it is concluded that DLC/ EGNSN coating on piston rings offered better resistance against wear than WC/ EGNSN coating.

Shaw et al. [18] studied the tribological behavior of diesel piston skirt coatings (Mn-P and polymer graphite) in CJ-4 and PC-11 engine oils. Experimental results revealed that CK-4 lubricant could replace the CJ-4 lubricant without wear penalty, but FA-4 lubricant may post a potential wear challenge. In the conformal contact, the Mn-P coating exhibited little friction benefit. But, in the point contact Mn-P coating exhibited detrimental impact on wear behavior of the piston skirt. However, in the conformal contact tests, the polymer-graphite composite coating decreased the friction by 15–30%, although the polymer-graphite coating caused a higher wear rate in the point contact sliding. This may be due to the Mn-P interlayer releasing hard particles after the top coat was worn through.

Liu et al [19] used the plasma spray process to deposit NiCrBSi coating on 304SS steel plates to investigate the microhardness, phase composition, microstructure and

Fig. 4 Tafel graphs of the coatings at (a) Chromium-coated rings, (b) Graphene oxide-chromium-coated rings (c) Scanning electron microscope image of the corroded surface of the chromium ring at 1M H₂SO₄, (d) Scanning electron microscope image of the corroded surface of graphene oxide-chromium ring at 1M H₂SO₄. Reprinted by permission from Elsevier: Elsevier, *Surface and Coatings Technology*, Wear and corrosion resistance enhancement of chromium surfaces through graphene oxide coating, Doğuş Özkan, Yaman Erarslan, Cem Kınçal, Oğuzhan Gürlü, M. Barış Yağcı, Copyright 2020, [16]



tribological characteristics of the as-sprayed coating. Further, the coating was heat-treated at a distinct temperature (300, 500 and 700 °C), respectively. The as-sprayed coating exhibited a dense structure (1.4%). In addition, the microhardness of the NiCrBSi coating is enhanced with increase in heat treatment temperature. The microhardness of the coatings after heat treatment at 300, 500 and 700 °C was measured to be 725, 891 HV_{0.1}, 1046 HV_{0.1}, respectively, as shown in Fig. 5.

Zhang et al. [20] studied the effect of molybdenum (Mo) addition on tribological characteristic of plasma-sprayed NiCrBSi coating on 304 SS substrate under dry and oil-lubricated environment. The Mo was added in NiCrBSi coating in distinct wt% (0, 5, 10, 20 and 30). The experimental results indicate that among all coatings, the 30 wt% Mo–NiCrBSi coating offered optimal wear and friction characteristics in both environments. This higher wear and tribological performance were owing to the formation of MoO₂ and MoS₂ tribofilms during friction process under oil-lubricated and dry environment. Except this, some hard phases were formed (Cr₁₃Ni₅Si₂, Cr₂B, Ni₃B and Cr₃C₂) as shown in Fig. 6. These hard phases help to increase hardness and result in higher wear rate.

Biberger et al. [21] analyzed the effect of test parameters (contact temperature, test duration, ring load and sliding speed) on the tribological behavior of hard chrome plated

on piston rings against Fe-based cylinder liner coating deposited by thermal spray process. The Fe-based coating was deposited on hypoeutectic aluminum–silicon alloy using twin wire arc spray process. Before the coating deposition, the liner surface was roughened using a high-pressure water jet to enhance roughness. This leads to high bond strength of the coating with the substrate (rough surface). The SEM image of thermal sprayed coating is shown in Fig. 7.

Figure 7a indicates the microstructure of the wire arc sprayed, Fe-based coating having 150 μm thickness on hypoeutectic aluminum–silicon alloy. The coating features involve pores and cavities, lamellar oxide skins as well as resolidified particles. Figure 7b shows the running surface of the liner. It depicts that the honing process opens the pores at the surface of the coating. However, Fig. 7c indicates the cross section. The friction was observed to be decreased rapidly with the increase in sliding speed at a load of 25N, owing to the increasing proportion of hydrodynamic lubrication. However, at 100 and 200N load, the coefficient of friction is not depending upon applied normal force.

Singh et al [22] evaluated the wear behavior of the CrN coating on piston ring (CI alloy) at lower load (10, 20, 30 and 40 N) and sliding velocity (0.3, 0.4, 0.6 and 0.8 m/sec.) under dry condition. The tribological test showed that with

Fig. 5 Bar graph indicating the micro-hardness value of plasma-sprayed NiCrBSi coating and heat-treated at different temperatures.

Reprinted by permission from Elsevier: Elsevier, *Surface and Coatings Technology*, Effect of heat treatment on structure and property evolutions of atmospheric plasma-sprayed NiCrBSi coatings, Liming Liu, Haifeng Xu, Jinkun Xiao, Xinlong Wei, GaZhang, Chao Zhang, Copyright 2017, [19]

Hardness of as sprayed and post heat treated samples

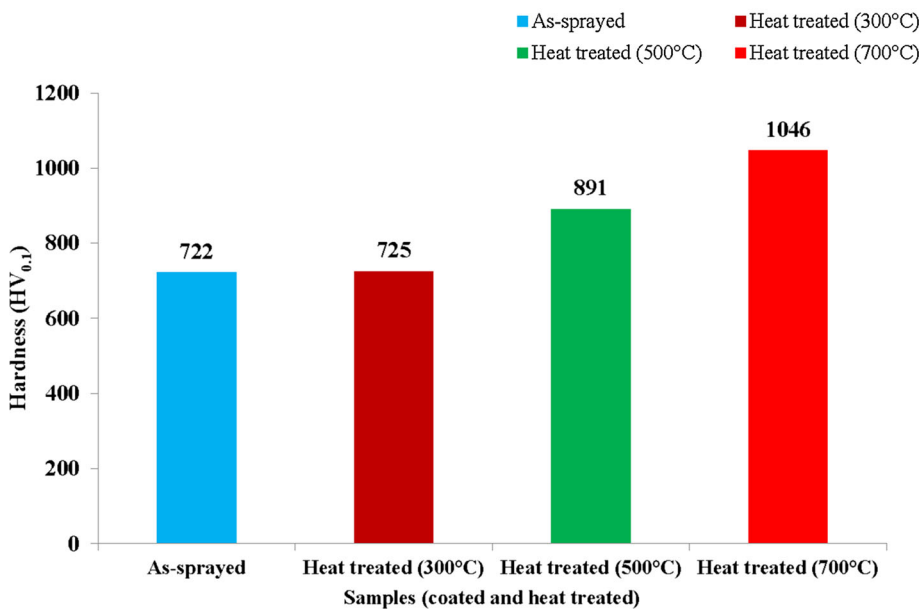
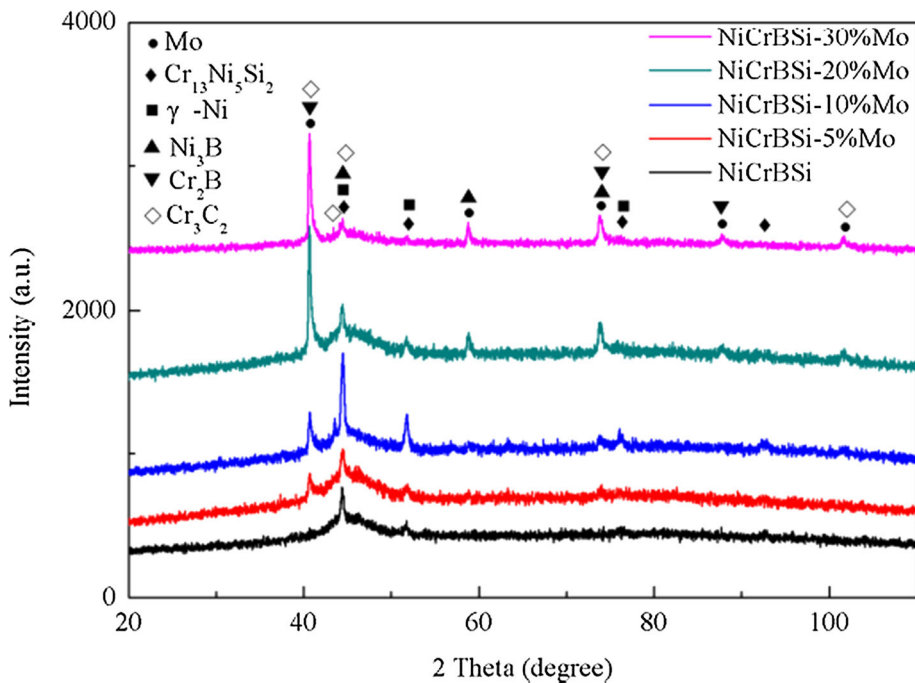


Fig. 6 XRD profile of the plasma-sprayed NiCrBSi and Mo-NiCrBSi composite coatings. Reprinted by permission from Elsevier: Elsevier, *Journal of Alloys and Compounds*, Role of Mo on tribological properties of atmospheric plasma-sprayed Mo-NiCrBSi composite coatings under dry and oil-lubricated conditions, Chao Zhang, Liming Liu, Haifeng Xu, Jinkun Xiao, GaZhang, Hanlin Liao, Copyright 2017, [20]



increase in load and velocity the specific wear rate decreased. This is owing to the fact that as the normal load increases the frictional heat develops because of increasing of temperature (from 28 to 42 °C) to the contact surface and hardening of wear surface, clogging, etc.

Pal et al. [23] reported that plasma-sprayed zirconia coating on aluminum substrate (piston head) enhances the efficiency and service life than alumina and titania ceramic powders.

Lin et al. [24] developed TiSiCN nano-composite coating on AISI304SS by using plasma enhanced magnetron sputtering process in distinct environment (N₂, Ar, C₂H₂ and hexamethyldisilazane (HMDSN). The microstructure and elemental composition of the TiSiCN nano-composite coatings were optimized by altering the flow rate of C₂H₂ and HMDSN. The optimized TiSiCN coating was achieved at a C₂H₂ flow rate of 20 sccm and HMDSN flow rate of 3 g/h. The results showed that a

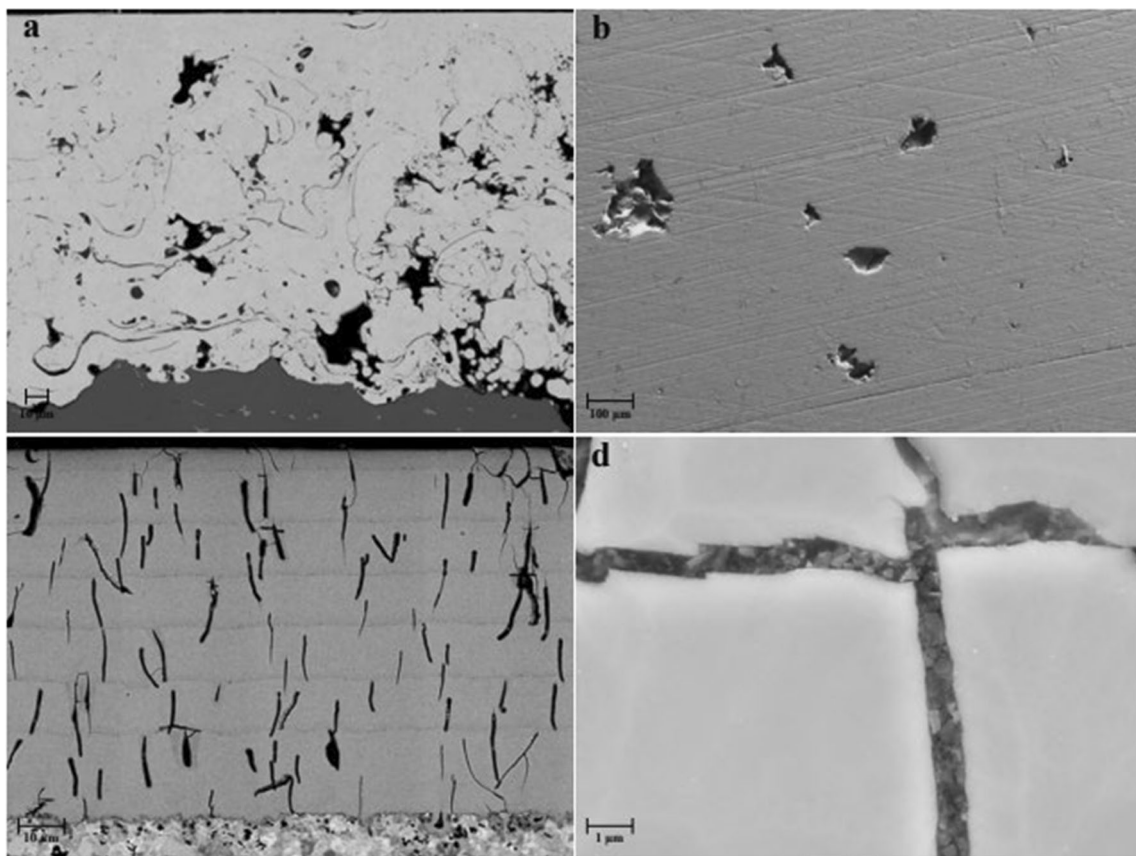


Fig. 7 Scanning electron images of (a) cross section of twin wire arc sprayed, nano-crystalline Fe-liner (SE) (b). Honed running surface of the twin wire arc sprayed, nano-crystalline Fe-liner (SE, through the lens) (c). The BSE image of a cross section of hard chrome-plated ring segment (d) Fe-polished cross section of hard chrome-plated ring segment with micro-cracks filled with diamond particles (SE).

Reprinted by permission from Elsevier: Elsevier, *Tribology International*, Development of a test method for a realistic, single parameter-dependent analysis of piston ring versus cylinder liner contacts with a rotational tribometer, Julian Biberger,Hans-Jürgen Füßer, Copyright 2017, [21]

significant reduction in wear rate and coefficient of friction of the coated rings was observed than the base steel under optimized conditions as shown in Fig. 8a and b.

Araujo et al. [25] examined the influence of periodicity on scratch resistance and hardness of CrN/NbN nanoscale multilayer coating on AISI4408 (piston ring) using PVD. For a periodicity of 4nm the coating exhibited maximum hardness (3200 HV). However, at 20nm periodicity coating showed the minimum critical load to coating failure, while 7.5nm and 4 nm periodicity coating showed the highest load. In simple words, lower the value of periodicity, the higher was the critical load to failure.

Lorenzo et al. [26] analyzed the effect of varying coating thickness (1, 5 and 10 μm) on the tribological behavior of chromium nitride (CrN)-coated H-13 steel under unidirectional sliding. The CrN coating deposited by PVD process with coating thickness (5 μm) exhibited optimal performance in terms of wear and friction. Also, CrN-3 coating having a 10 μm coating thickness exhibited better

tribological characteristics than coating having 1 μm coating thickness.

Igartua et al. [27] used high-velocity oxy fuel (HVOF), PVD and electrolytic composite coatings (nano-75Cr₃C₂-25NiCr, WCCoCr/CrC-NiCr, 75Cr₃C₂-25NiCr, NiP-CO+Si₃N₄, CrN/TiN and Cr) on piston rings and simulated tests were conducted. The result showed that nano-HVOF sprayed CrC75-NiCr25 coating, the PVD (TiN/Ti-CrN/Cr) coatings and the NiPCO+Si₃N₄ coating enhanced the wear and friction performance in relation to the Cr coatings. Among all coatings CrN/TiN PVD coating exhibited the lowest wear rate.

Houdkova et al. [28] deposited Cr₃Cr₂-25%NiCr coating on carbon steel (CSN11523) using a HVOF spray process. Further, pin on disk test was performed on as-sprayed coating to examine the sliding wear performance under distinct test environment. Tribological test results showed that Cr₃Cr₂-25%NiCr coating causes more coefficient of friction than Cr₃Cr₂-25%NiCr coating Al₂O₃. In addition,

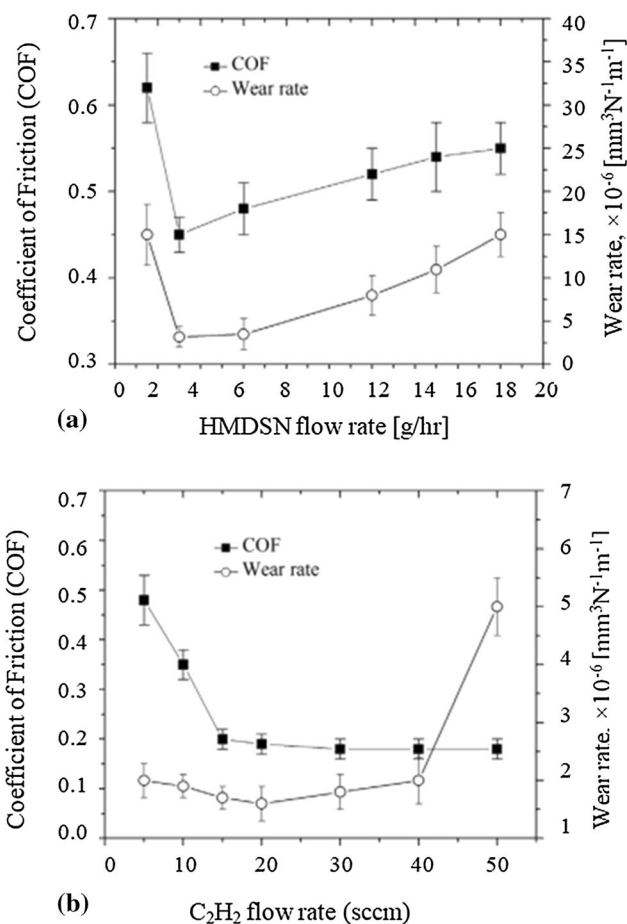


Fig. 8 Dry sliding coefficient of friction and wear rate of coatings sliding against SS316 balls (a) Group-1 TiSiCN coatings sprayed at a distinct flow rate of HMDSN (b) Group -2 TiSiCN coatings sprayed at a distinct flow rate of acetylene

the coefficient of friction (COF) decreases with the rise in test temperature. However, the COF reduces more than 5 times when lubricant is present.

Jang et al [29] studied the effect of hardness of the piston ring coatings: 74%Cu-17% Al (soft coating) and Cr-Al oxide (hard coating) on the wear properties of rubbing surfaces. The material utilized for engine cylinder liner was gray C.I. has a coarse flake graphite microstructure with average hardness of 300 HV. The average hardness of Cu-Al and Cr-Al coating was measured to be 143.7HV and 719.6 HV, respectively. Further, the wear test was conducted on pin on disk testing machine at distinct parameters (roughness, temperature and lubrication). From the result, it is clear that the friction coefficient and the wear rate of Cu-Al coating were higher than Cr-Al oxide coating.

Cho et al. [30] analyzed the effects of graphite and diamond-like carbon coatings and surface roughness on the tribological performance of the piston skirt (gray cast iron). Experimental results showed that the friction coefficient of

the graphite and diamond-like carbon (DLC) coating was higher than graphite coating. In addition, the graphite coating was not effective in safeguarding the wearing of the surfaces. However, the DLC coating offered much better tribological properties as compared to graphite coating.

Skopp et al. [31] deposited atmospheric plasma-sprayed $\text{Ti}_n\text{O}_{2n-1}$ coating and vacuum plasma-sprayed $\text{TiO}_{1.95-x}$ coating on gray cast iron (GG20HCN). Further, the tribological behavior of both coatings was compared under lubricating conditions. Both the coatings showed a low porosity (about 2%) and excellent adherence and hardness (785 to 846HV_{0.2}).

Karamiš et al. [32] evaluated the frictional forces and surface characteristic developed from plasma-sprayed Al-Mo-Ni-coated piston ring (AISI440C steel). The test was conducted under distinct temperature (25, 100, 200 and 300 °C), load condition (83N, 100N, 200N and 300N) and environment (dry and lubricating). In dry conditions, the surface roughness was found to be increased with an increase in load. However, the surface roughness increased with increase in temperature up to 200 °C and after that it starts decreasing. But, in lubricating condition, the less roughness was obtained at the same temperature. Further, it was observed that under lubricated friction conditions, there is no systematic relationship between test temperature and roughness. However, at 200 °C small variations in surface roughness were observed, because it is the lowest value at this temperature, although the variation of frictional forces w.r.t. sliding distances during dry and lubricated conditions is depicted in Figs. 9 and 10, respectively.

Figure 9 shows that under dry condition, the frictional forces generally increased with sliding distance up to around 100 m. However, frictional force reached steady-state regime with a sliding distance of 100 m. These stable tendencies were found at load of 83N, 100N & 200N. However, the decrease in frictional forces after running in period went on continuously under test load of 300N as depicted in Fig. 9d.

However, in case of Fig. 10a to d similar results under lubricated conditions to those attained under dry conditions were observed. But the frictional forces are less in case of lubricating condition than dry condition. In addition, the as-sprayed coating offered lower hardness value as compared to AISI440C steel. However, at coating–substrate interface maximum hardness was observed (500HV_{0.04}).

Bemporad et al [33] adopted multilayer CrN/NbN coating and deposited on the piston ring (X82WMoV65) to examine the microstructure, composition, morphology and tribological properties of the nanoscale multilayer coating. The CrN/NbN coatings exhibited lower wear rate than CrN coating (up to 30%). Overall, CrN/NbN coatings on piston

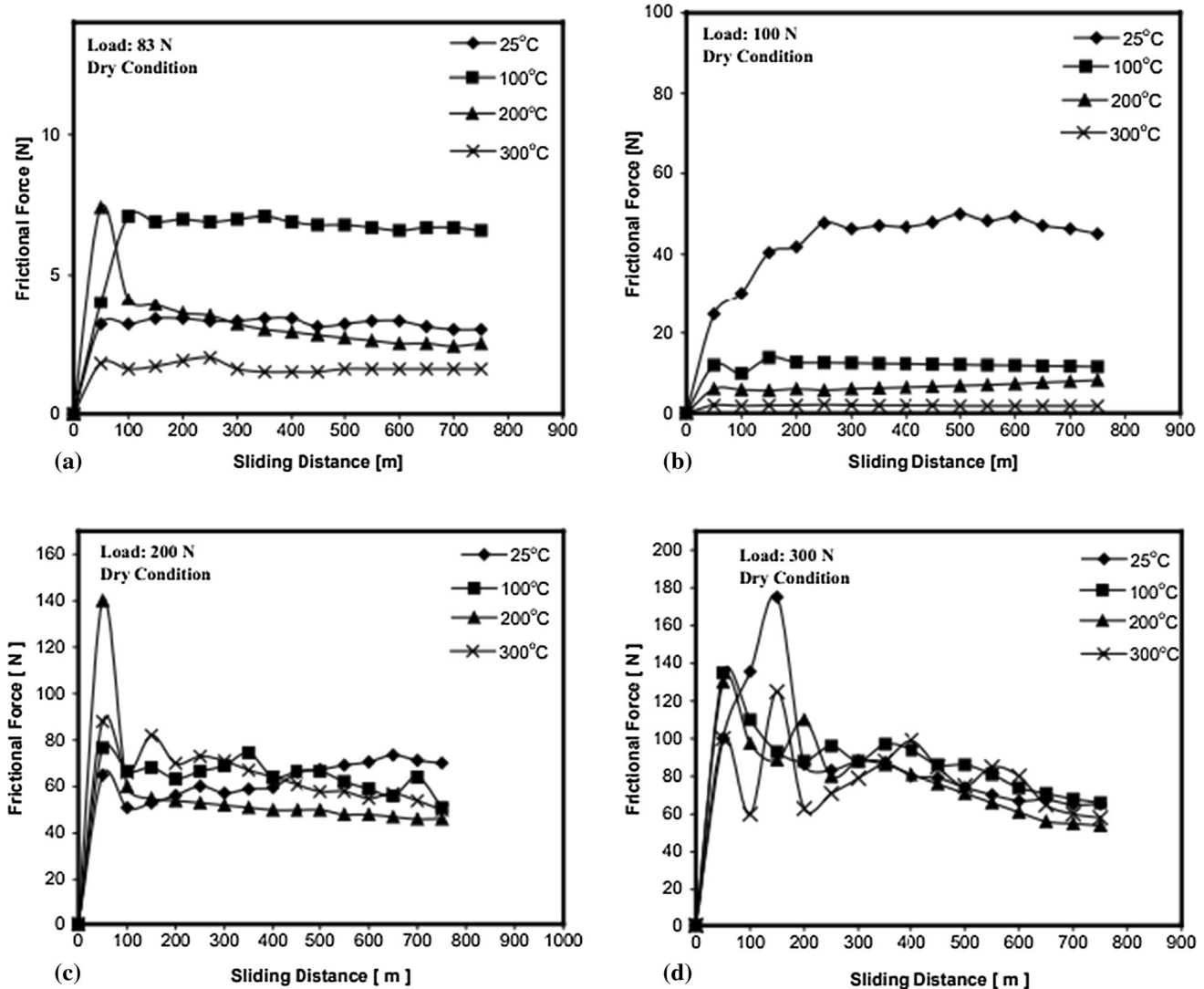


Fig. 9 Variation of frictional forces w.r.t. sliding distance under dry conditions at different load conditions (a) Load =83N (b) Load=100N (c) load=200N (d) 300N. Reprinted by permission from Elsevier:

Elsevier, *Applied Surface Science*, An evaluation of surface properties and frictional forces generated from Al-Mo-Ni coating on piston ring, M.B Karamış, K Yıldızlı, H Çakırer, Copyright 2004, [32]

ring enhance the performance of the component by 30% than CrN coating and improved lifetime from 9 to 11 months. Zhuo et al. [34] deposited multilayer compound coating (Ti-TiN) up to 4 μm thickness on the CI piston ring using magnetron sputtering ion compound and multi-arc technique. The results showed that the resistance against wear of multi-layer coating increases with increasing number of layers. Friedrich et al. [35] used PVD to deposit Cr_xN coating on piston rings (DIN 1.4112 steel) to study their tribological behavior. The cross-sectional SEM image of coating morphology is shown in Fig. 11.

Figure 11 indicates that coatings exhibited columnar structure. In addition, the coating showed higher hardness, adequate adhesion, and moderate compressive residual

stresses. The result showed that the PVD hard coating can reduce wear rates very effectively.

Finally, the results of past research are summarized in Table 2 and shown graphically from Figs. 12, 13, 14, 15 and 16.

From Fig. 12, H-13 steel coated with CrN material using physical vapor deposition methods produces least roughness, while Gray cast iron coated with graphite and diamond-like carbon (DLC) produces maximum roughness [26, 30].

From Fig. 13, the polymer matrix [18], Zirconia+NiCrY coating [23] and gray cast iron coated with Cu-Al coating using a physical vapor deposition process [29] offered less hardness, while the NbN/CrN coating deposited on AISI4408 using PVD provides maximum hardness [25].

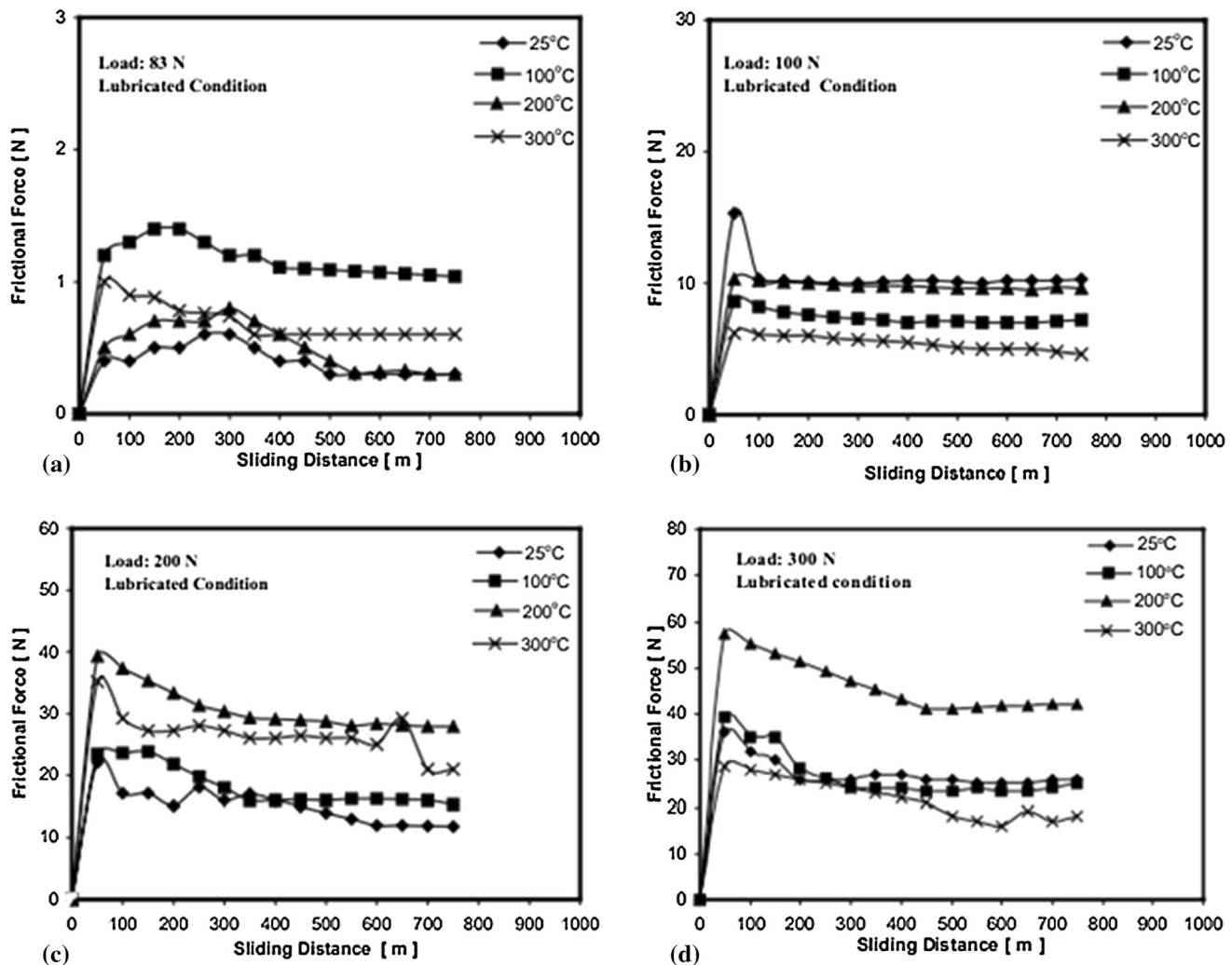


Fig. 10 Variation of frictional forces w.r.t. sliding distance under lubricated conditions at different load conditions (a) Load = 83 N (b) Load = 100 N (c) load = 200 N (d) 300 N. Reprinted by permission from Elsevier: Elsevier, *Applied Surface Science*, An evaluation of surface properties and frictional forces generated from Al-Mo-Ni coating on piston ring, M.B Karamış, K Yıldızlı, H Çakırer, Copyright 2004, [32]

From Fig. 14, AISI304SS coated with TiSiCN using a PVD process gives the least elastic modulus (GPa), while the X82WMoV65 tool steel coated with CrN or CrN/ NbN material by using a cathode switching reactive cathodic arc evaporative method gives maximum elastic modulus value [24, 33].

From Fig. 15, Piston ring and CI cylinder coated with diamond-like carbon (DLC) using physical vapor deposition process have least COF, while H-13 steel coated with CrN-1 material using PVD process have maximum COF [17, 26].

From Fig. 16, cast iron coated with diamond-like carbon using PVD offered least wear rate, while the TiSiCN coating deposited on AISI304SS material offered maximum wear rate [17, 24].

Coating deposited by PVD process offers better wear and friction properties. However, plasma-sprayed Mo/Cr

carbide and plasma-sprayed Cr oxide piston face coatings exhibited higher resistance against wear than plasma-sprayed Mo or Mo carbide and electroplated Cr. For piston ring, low-pressure plasma-sprayed ceramic metal composite coating offered better wear-resistant properties. In addition, HVOF sprayed CrC–NiCr can be used in place of hard Cr coating depending upon various factors such as COF, cost and environmental issues [36].

Causes and Possible Solutions

The failure of engine piston and skirt due to fatigue (mechanical, thermal and mechanical fatigue) is one of the main reasons. The crack initiates in the vertical plane that comprises a pinhole. Further, this crack propagates up to the piston crown. This may be due to the static stress

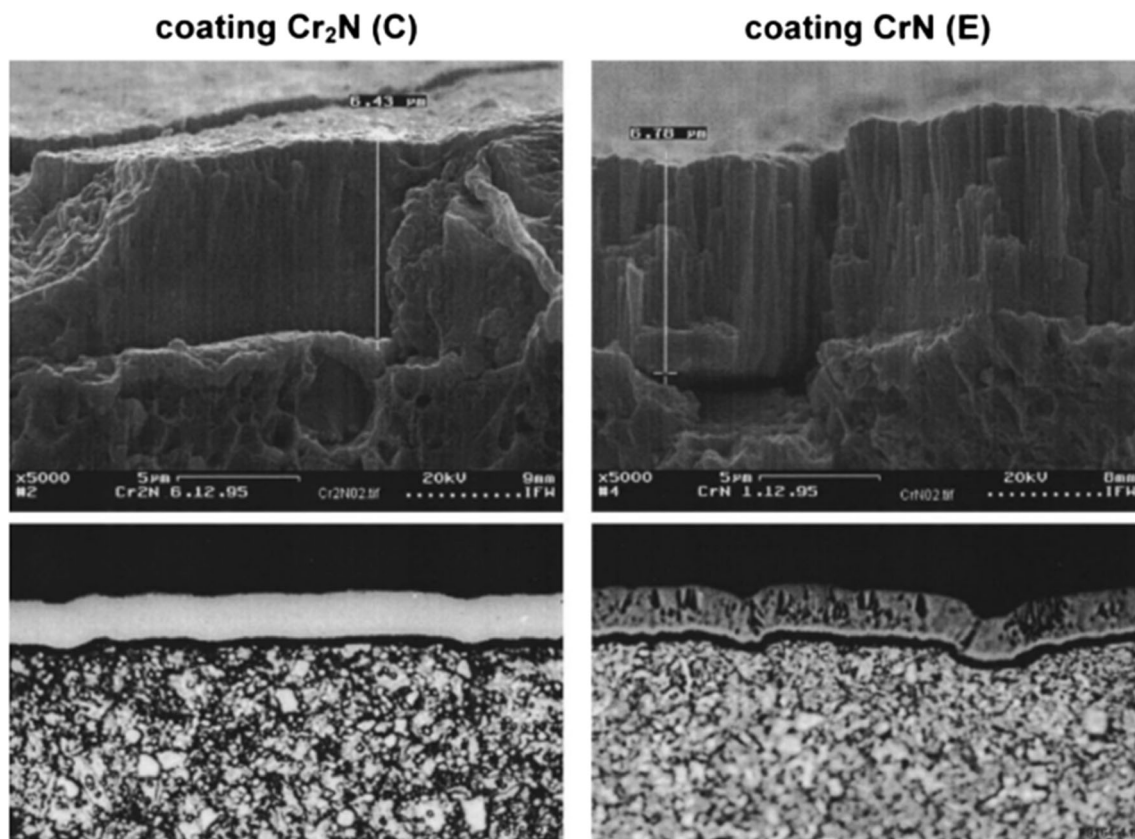


Fig. 11 Cross-sectional SEM image of PVD coatings (Cr_2N) and (CrN). Reprinted by permission from Elsevier: Elsevier, *Surface and Coatings Technology, PVD Cr x N coatings for tribological*

application on piston rings, C Friedrich,G Berg,E Broszeit,F Rick,J Holland, Copyright 1997, [35]

concentration at the piston pinhole as shown in Fig. 17. But sometimes, the cracks initiate at the head as shown in Fig. 18.

The reasons for crack propagation at the head may be due to temperature and fatigue (mechanical/thermal). As during engine working, the high temperature is produced in the combustion chamber. Thus, the piston head is always hotter as compared to the bottom part and pinhole area. Due to this, the resistance against fatigue of the material at the piston head lower [38–42]. Other reasons for piston failure are high clearance b/w the piston and cylinder wall. This may be owing to the wear of the cylinder wall. Thus, high pressure act on compression ring which results in crack propagation. In addition, the high clearance permits the piston to rotate and to contact the cylinder wall at two points (top of piston head, bottom part of the skirt). This may also lead to introducing a flexural load on piston skirt and results in failure [43, 44]. To solve these issues (piston failures due to fatigue) some measures are given as shown in Fig. 19.

Material Selection

Piston material should have the ability to withstand very high temperature and have high resistance against mechanical and thermal fatigue. New alloy with silicon and copper content can be used [45, 46].

However, the metal matrix composites (MMCs) have been employed by many researchers in past [47–49]. However, various researchers are working on enhancing the material properties by die-casting processes [50, 51]. The advancement of new materials & processing technologies having higher fatigue and high-temperature mechanical performance would be useful to minimize the piston failure due to fatigue.

Surface Modification (By Applying Coating)

Coating on the piston is an effective way to reduce wear, friction and operating temperature. It increases the torque,

Table 2 Summary of distinct coatings material deposited on piston rings and piston by distinct coating process

S. No.	Authors	Years	Piston/Cylinder Liner/Piston Ring Material	Coating Material	Coating Process	Wear Testing / Environment	Testing condition and test parameters
1	Ozkan et al. [16]	2020	Cr-coated steel (Piston ring)	Graphene oxide	PVD	Tribological test / (lubricated condition)	Used commercial tribometer, Load = 60N, Sliding distance = 72.6 m, Temperature = 100±2 °C, Sliding speed = 0.055 m/s, Humidity = 40%, Minimum oil thickness = 63.3 mm, Lambda ratio =0.18, Max. Contact pressure =0.19 GPa.
2	Kumaret al. [17]	2018	Piston ring and CI cylinder liner	Diamond-like-carbon (DLC) Tungsten carbide (WC)	PVD method	Tribological test under firing engine environment, Dry & base oil (SN150) lubricated conditions	Test was performed by running by running the single cylinder, constant speed, 4-stroke diesel engine (Kirloskar Oil Engines Limited/ DM 10) at 1500 rpm and 50% rated load condition for 4 h.
3	Shaw et al. [18]	2017	38Mn-SiVSS steel	Mn-P Polymer graphite	screen print followed by a curing process	Wear test (conformal and point-contact) / lubricating condition	Tribological test was conducted on reciprocating tribometer in both the conformal and point-contact configurations. Normal load= 240 N oil temperature = 100 °C, oscillation frequency = 10 Hz, stroke length = 10 mm, total sliding distance =1000 m.
4	Liu et al. [19]	2017	304SS	NiCrBSi	Atmospheric Plasma spray	Tribological test on Ball on Disk configuration (dry condition)	The tribological tests parameter were: Load = 10N, Reciprocating frequency = 2 Hz, Stroke length = 8mm, Sliding velocity = 32mm/s, Sliding time = 4 hr, Temperature = 20°C
5	Zhang et al. [20]	2017	304SS	NiCrBSi 5%Mo-NiCrBSi 10%Mo-NiCrBSi 20%Mo-NiCrBSi 30%Mo-NiCrBSi	Atmospheric Plasma spray	Tribological test / Dry and lubrication (SAE 5W-40) condition	The reciprocating friction tests were conducted on a tribometer (UMT-2), Dia. of Si ₃ N ₄ ball = 4mm, Load = 10N, Sliding speed = 64mm/s, Stroke length = 8mm, total friction length = 460m.
6	Biberger et al. [21]	2017	Steel 1.4112	(X90CrMoV18)	Diamond reinforced hard chrome plated	Thermal Sprayed	Rotational sliding friction and wear tribometer (TE47)

Maximum speed of
motor =4000 rpm,
Sliding speed =
17.4 m/s,
Diameter of liner
bore =83 mm.

Table 2 continued

S. No.	Authors	Years	Piston/Cylinder Liner/Piston Ring Material	Coating Material	Coating Process	Wear Testing / Environment	Testing condition and test parameters
7	Singh et al. [22]	2017	Cast iron alloy	CrN	PVD (Cathodic arc evaporation)	Wear test (Pin on disk)/ Dry condition at room temperature	Load = 10, 20, 30 and 40 N, Sliding distance = 1000 m, track dia. = 60, 50, 40 and 30, respectively.
8	Pal et al. [23]	2017	Aluminum	Zirconia (thermal barrier coating)+ bond coat (NiCrAlY)	Plasma spray	Salt spray test/ alkaline environment	Salt spray test parameter: Temperature of chamber =34.5 to 35.5°C, pH value = 6.65 – 6.85, Solution concentration = 4.80 – 5.30% of NaCl, Air pressure = 14–18 psi, Quantity of salt solution collected = 1.0 – 1.5 ml/hr.
9	Lin et al. [24]	2016	AISI304SS	TiSiCN (G1-1) TiSiCN (G1-2) TiSiCN (G1-3) TiSiCN (G1-4) TiSiCN (G1-5) TiSiCN (G1-6) TiSiCN (G2-1) TiSiCN (G2-2) TiSiCN (G2-3) TiSiCN (G2-4) TiSiCN (G2-5) TiSiCN (G2-6) TiSiCN (G2-7)	PVD (Plasma enhanced magnetron sputtering)	Dry ball-on-disk test and TE77 test/ ambient air	Diameter of grade 5 SS316ball = 6.35 mm, Surface roughness = 25nm, Load = 1N, Sliding speed = 6.5 cm/s, travel length = 377m.
10	Araujo et al. [25]	2015	AISI4408 (piston ring)	NbN/CrN (20nm) NbN/CrN (10nm) NbN/CrN (7.5nm) NbN/CrN (4nm)	PVD (Cathodic arc physical vapor deposition)	Scratch and Hardness Test	Scratch tests were performed in a CSM, model REVETEST Xpress. Indenter = Diamond, Cone angle = 120 degree, tip radius = 100μm, Speed = 4mm/min., Load = 0 to 180N.
11	Lorenzo et al. [26]	2013	H-13 steel	CrN-1 CrN-2 CrN-3	PVD (Plasma enhanced magnetron sputtering)	Friction and wear test (by using a ball-on-flat configuration)	Load = 5, 10, and 20 N, Pressure = 1.07, 1.15, and 144 GPa, Diameter of WC ball = 1/2 inch, Roughness (Ra) = 0.038 μm.
12	Igartua et al. [27]	2011	Cast Iron (cylinder liner)	Nano-75Cr ₃ C ₂ -25NiCr Power size -10 μm WC CoCr/CrC-NiCr Power size -30+10μm 75Cr ₃ C ₂ -25NiCr Power size -45 +20μm NiPCO+Si ₃ N ₄ CrN/TiN	HP-HVOF HP-HVOF HP-HVOF Electrolytic PVD	Friction and wear test/mixed lubricated condition	SRV test rig was used under distinct condition (linear, oscillating sliding motion for mixed lubricated conditions), Load = 300N, time = 30s, using slow ramp speed rate.

Table 2 continued

S. No.	Authors	Years	Piston/Cylinder Liner/Piston Ring Material	Coating Material	Coating Process	Wear Testing / Environment	Testing condition and test parameters
13	Houdkova et al. [28]	2010	Carbon steel (CSN11523)	Cr ₃ Cr ₂ -25%NiCr	Thermally sprayed (HVOF coating)	Sliding wear test (pin on disk test) under lubricated condition	Load = 10N, Speed = 0.1m/s.
14	Jang et al. [29]	2009	Gray cast iron (cylinder liner)	Cu-Al Cr-Al oxide	...	Wear test (Pin on disk)/ lubricating condition	Dia. of disk = 54.9mm, height = 6mm, wear test was conducted using POD testing system, for 1 hour and at distinct temperature (25°C, 100°C, 170°C and 230°C)
15	Cho et al. [30]	2009	Gray cast iron	Graphite Graphite & diamond-like carbon (DLC)	PVD	Wear test/ lubricating condition	Reciprocating wear tester was used, Load = 200N, Frequency =2 Hz, time =3 hrs.
16	Skopp et al. [31]	2007	gray cast iron GG20HCN	Mo (MKP81A) Ti _n O _{2n-1} (n=4-6) (Ti, Mo)(C,N) + 23NiMo (TM23-1) WC/Cr ₃ C ₂ -based	Atmospheric Plasma Spray Atmospheric Plasma Spray Atmospheric Plasma Spray HVOF	Wear test DIN 50324 (ASTM G-99) /mixed lubrication and dry-running conditions	Load = 10N, Pressure = 1000MPa, Sliding distance = 5000m, Temperature = 22 and 400°C, sliding speed = 1m/s.
17	Karamiç et al. [32]	2004	AISI 440C steel (Piston Ring)	Al-Mo-Ni	Plasma spray method	Sliding Wear (dry & lubricated test conditions)	Sliding speed = 1m/s, For frictional response of coating, temperature = 25°C, 100°C, 200°C, and 300°C; Load = 83N, 100N, 200N and 300N was applied.
18	Bemporad et al. [33]	2004	X82WMoV65 tool steel	CrN/NbN CrN	cathode switching reactive cathodic arc evaporative method	Ball-on-ring wear test	The resistance against abrasive wear was measured by (a) Rotating Wheel Abrasive Wear Test: Dia. of steel wheel = 15mm, speed = 200 rpm, load = 0.6N (b) Micro-Abrasion Wear Testing system: Diameter of steel sphere = 30mm, speed = 100 rpm
19	Zhuo et al. [34]	2000	C I piston ring	Ti-TiN (Three layer) Ti-TiN (five layer) Ti-TiN (Seven layer) Ti-TiN (Nine layer)	Multi-arc & magnetron sputtering ion compound plating	Simulative non-lubrication wear machine	Author developed simulative non-lubrication wear machine to measure the wear-resistant properties of the piston ring,
20	Friedrich et al. [35]	1997	Steel DIN 1.4112	Cr _x N	PVD (magnetron sputtering)	Ring-on-disk model-wear tests / lubricating condition	Load = 50N, Distance = 720m and time = 20 hours.

Table 2 continued

S. No.	Authors	Years	Piston/Cylinder Liner/Piston Ring Material	Coating Material	Coating Proces Elastic modulus	Wear Testing / Environment	Testing condition and test parameters
S. No.	Speed (rpm)/load/cycle	Coating thickness (μm)	Roughness	Hardness	COF of coating	Wear rate of coating	
1	...	100 μm	$R_a = 162 \text{ nm}$ and $R_q = 214 \text{ nm}$	16 GPa	275 GPa	0.12	...
2	1500/50% rated engine load/3.6×10 ⁵ cycles (4 hours duration)	50 to 60 μm	1350 nm	180 to 285 HV (for cylinder liner)	...	0.05–0.07	$1.69 \times 10^{-12} \text{ mm}^3/\text{N}\cdot\text{m}$ (for top ring)
							$2.31 \times 10^{-12} \text{ mm}^3/\text{N}\cdot\text{m}$ (for middle ring)
							$2.11 \times 10^{-12} \text{ mm}^3/\text{N}\cdot\text{m}$ (for top ring)
							$2.86 \times 10^{-12} \text{ mm}^3/\text{N}\cdot\text{m}$ (for middle ring)
3	Load = 240N	3-5 μm	2910 nm	100–200 HV	0.12	...	
		3–4 μm (top coat 15–17 μm)		30–35HV	0.08		
4		350 μm		728 HV _{0,1}	0.63–0.70		$1.1 \times 10^{-5} (\text{mm}^3/\text{N}\cdot\text{m})$
5	64mm/sec.	100–150 μm		$903.6 \pm 59.7 \text{ HV}_{0,1}$	0.69 (dry condition) and 0.103 (lubricating condition)		$4360 \mu\text{m}^3/\text{N}\cdot\text{m}$ (dry condition) and $235 \mu\text{m}^3/\text{N}\cdot\text{m}$ (lubricating condition)
				$765.1 \pm 106 \text{ HV}_{0,1}$	0.67 (dry condition) and 0.100 (lubricating condition)		$3700 \mu\text{m}^3/\text{N}\cdot\text{m}$ (dry condition) and $175 \mu\text{m}^3/\text{N}\cdot\text{m}$ (lubricating condition)
				$755 \pm 106 \text{ HV}_{0,1}$	0.65 (dry condition) and 0.095 (lubricating condition)		$3500 \mu\text{m}^3/\text{N}\cdot\text{m}$ (dry condition) and $45 \mu\text{m}^3/\text{N}\cdot\text{m}$ (lubricating condition)
				$720 \pm 106 \text{ HV}_{0,1}$	0.63 (dry condition) and 0.090 (lubricating condition)		$2900 \mu\text{m}^3/\text{N}\cdot\text{m}$ (dry condition) and $20 \mu\text{m}^3/\text{N}\cdot\text{m}$ (lubricating condition)
				$683.1 \pm 63.9 \text{ HV}_{0,1}$	0.61 (dry condition) and 0.088 (lubricating condition)		$1287 \mu\text{m}^3/\text{N}\cdot\text{m}$ (dry condition) and $10 \mu\text{m}^3/\text{N}\cdot\text{m}$ (lubricating condition)
6	4000 rpm	78 μm	-	$10.1 \pm 2.1 \text{ GPa}$	$272 \pm 47 \text{ GPa}$	$0.055–0.12$	7.5mm/hour

Table 2 continued

S. No.	Authors	Years	Piston/Cylinder Line/Piston Ring Material	Coating Material	Coating Proces	Wear Testing / Environment	Testing condition and test parameters	
7	96 rpm	13 μm	0.20	11.90 mm ³ /Nm	
	153 rpm					0.15	3.2 mm ³ /Nm	
	287 rpm					0.16	3.96 mm ³ /Nm	
	510 rpm					0.27	1.1 mm ³ /Nm	
8	...	300 μm	6502 nm 20 nm	54.73 HV	15×10 ⁶ mm ³ /Nm	
9	6.5 cm/sec, 1 N and 10, 000 cycles.	17.5 μm 11.1 μm 19.5 μm 20.1 μm 19.6 μm 13.1 μm 20 μm 16.5 μm 13.5 μm 14.4 μm 16.5 μm 10.1 μm 19.5 μm 25–30 μm	27.5GPa 29GPa 26GPa 23GPa 21GPa 8GPa 21GPa 17GPa 15GPa 14GPa 13GPa 12.5GPa 12.5GPa 2000HV 2800HV 3000HV 3200HV	330GPa 350 GPa 310 GPa 315 GPa 305 GPa 150 GPa 300 GPa 255 GPa 225 GPa 180 GPa 150 GPa 130 GPa 130 GPa 2000HV 2800HV 3000HV 3200HV	0.62 0.46 0.48 0.52 0.54 0.56 0.47 0.35 0.20 0.19 0.18 0.17 0.16 0.30 0.19 0.18 0.19	...	3.2×10 ⁻⁶ mm ³ /Nm 3.4×10 ⁻⁶ mm ³ /Nm 8×10 ⁻⁶ mm ³ /Nm 11×10 ⁻⁶ mm ³ /Nm 15×10 ⁻⁶ mm ³ /Nm 2×10 ⁻⁶ mm ³ /Nm 1.9×10 ⁻⁶ mm ³ /Nm 1.7×10 ⁻⁶ mm ³ /Nm 1.6×10 ⁻⁶ mm ³ /Nm 1.8×10 ⁻⁶ mm ³ /Nm 2×10 ⁻⁶ mm ³ /Nm 5×10 ⁻⁶ mm ³ /Nm
10								
11	1cm/sec, load (5,10 and 20N) and 60 min.	1 μm 5 μm 10 μm 0.15mm 0.19mm 0.13mm 15 μm 8.5 μm 0.145 mm	11 nm 25 nm 24 nm 110 nm 330 nm 230 nm 240 nm 170 nm 1200 nm 433 ± 9 μm	18 GPa 12 GPa 16.5 GPa 801HV 1039 HV 798 HV 1057 HV 1965 HV 1136 HV 1030 ± 114 HV _{0.3}	220 GPa 180 GPa 220 GPa 801HV 1039 HV 798 HV 1057 HV 1965 HV 1136 HV 1030 ± 114 HV _{0.3}	0.2 to 0.8	
12	Load = 300N					
13	0.1m/s, load (10N) and 50000 cycles					0.62 ± 0.04		

Table 2 continued

S. No.	Authors	Years	Piston/Cylinder Line/Piston Ring Material	Coating Material	Coating Proces	Wear Testing / Environment	Testing condition and test parameters
14	Speed = 2.75 m/s, load = 100N	0.25mm to 0.35mm 0.3mm to 0.4mm 2 μ m	7500–8000 nm 280–350 nm 1740–5120 nm	143.7HV 719.6HV	...	0.34 0.29 0.1–0.13	48×10^{-5} mm ³ /mm 2.2×10^{-5} mm ³ /mm
15	Speed = 0.5Hz, Load = 50N and 700N for 3 hours	100–300 μ m	500 nm	566 HV _{0.2}	
16	1m/sec, load (10N) for dry condition while speed = 0.3m/s, load (50N)	100–300 μ m	500 nm 3100 nm 110 nm	657 HV _{0.2} 699 HV _{0.2} 1200 HV _{0.2}	
17	Sliding speed: 1m/sec, load = 83, 100, 200 and 300 N and cycle = 2	550 to 700 μ m	...	200–500 HV _{0.04}	
18	Speed: 200 rpm, load = 0.6 N	3.6 μ m 3.8 μ m 4–5 μ m	30 nm 60 nm ...	1690 HV ₅₀ 1755 HV ₅₀ 14.86 HMV _{0.01} (GPa) 18.03 HMV _{0.01} (GPa) 20.39 HMV _{0.01} (GPa) 21.90 HMV _{0.01} (GPa)	246–460 GPa 238–320 GPa ...	0–0.65 0–0.52 ...	9107 μ m ³ /mm N 7648 μ m ³ /mm N
19							
20	Speed = 0.01m/s, load = 50N and cycle =	6–8 μ m	180–350 μ m		0.20		

*R_a=arithmetic roughness value, R_q=root-mean-square value.

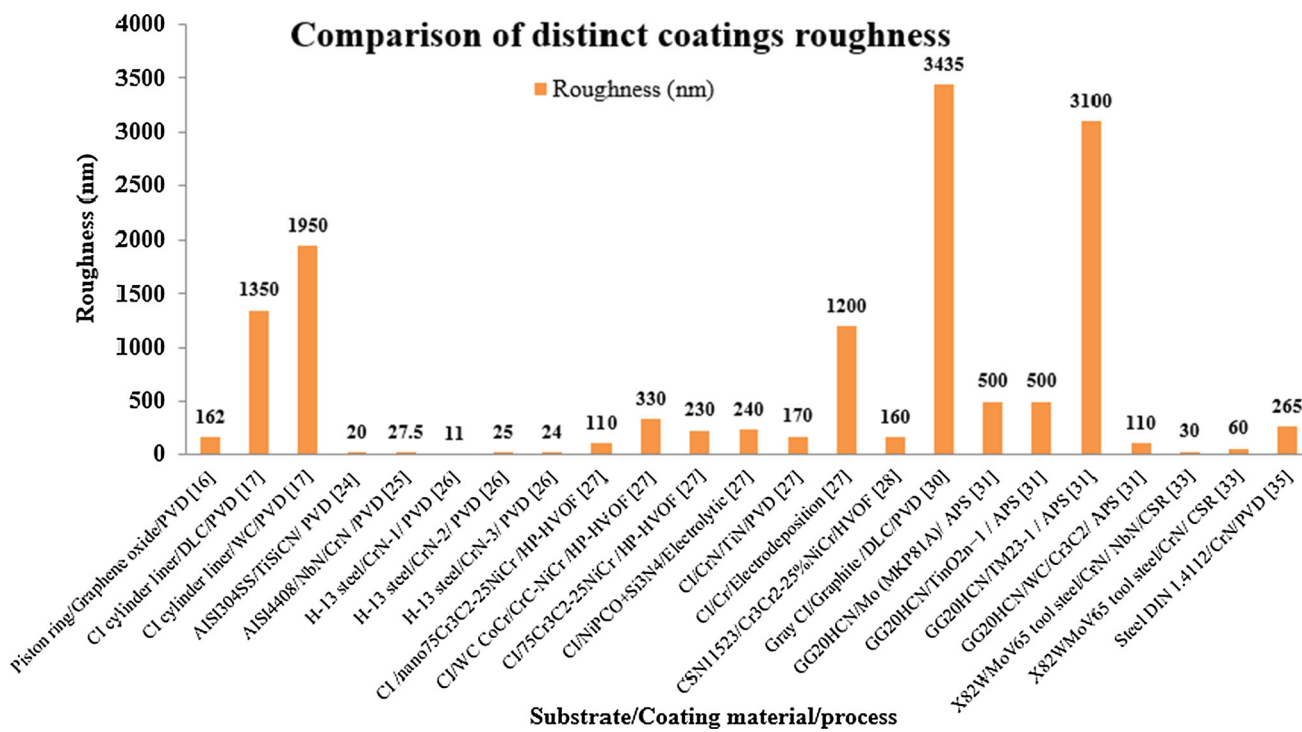


Fig. 12 Coating roughness (nm) Vs. substrate/coating/process by distinct processes on piston/cylinder liner materials

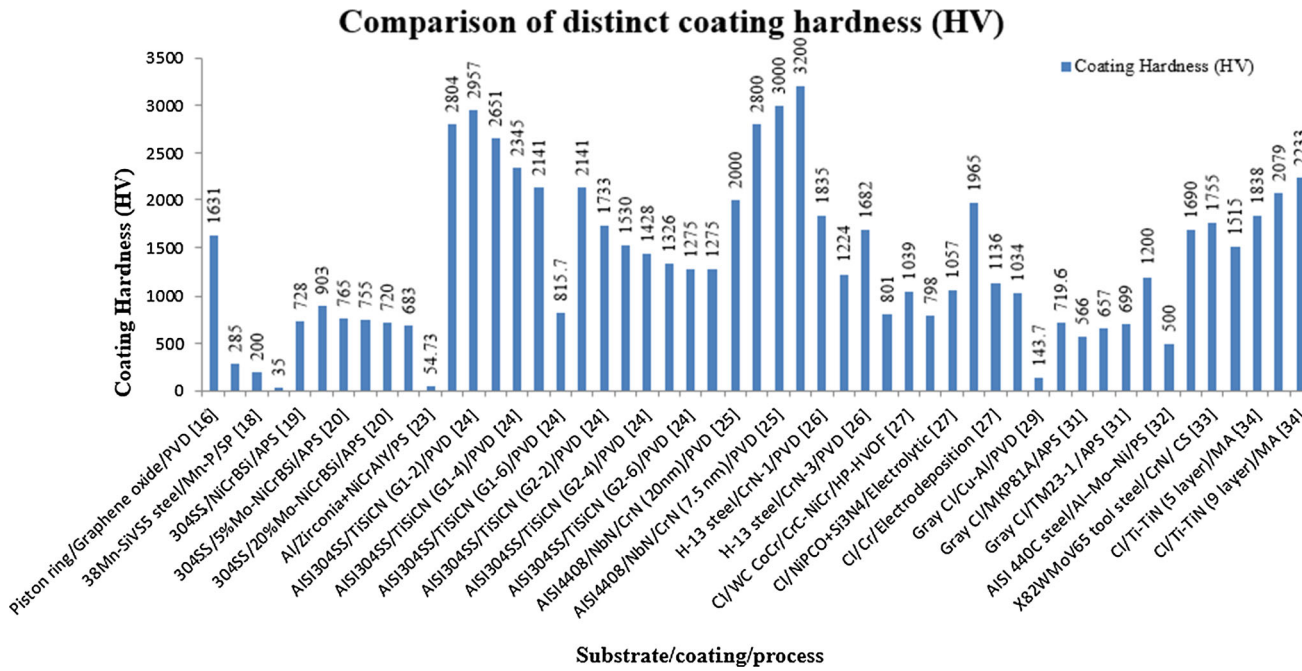


Fig. 13 Coating hardness (HV) Vs. substrate/coating/process by distinct processes on piston/cylinder liner materials

horsepower, decreases or eliminates detonation, allows a high compression ratio to be used and provides a better ring seal. In addition, coating plays an effective role to combat corrosion and oxidation at high temperature [52–56].

Further, distinct coating and process that can enhance the tribological and wear performance of piston are summarized in Table 2.

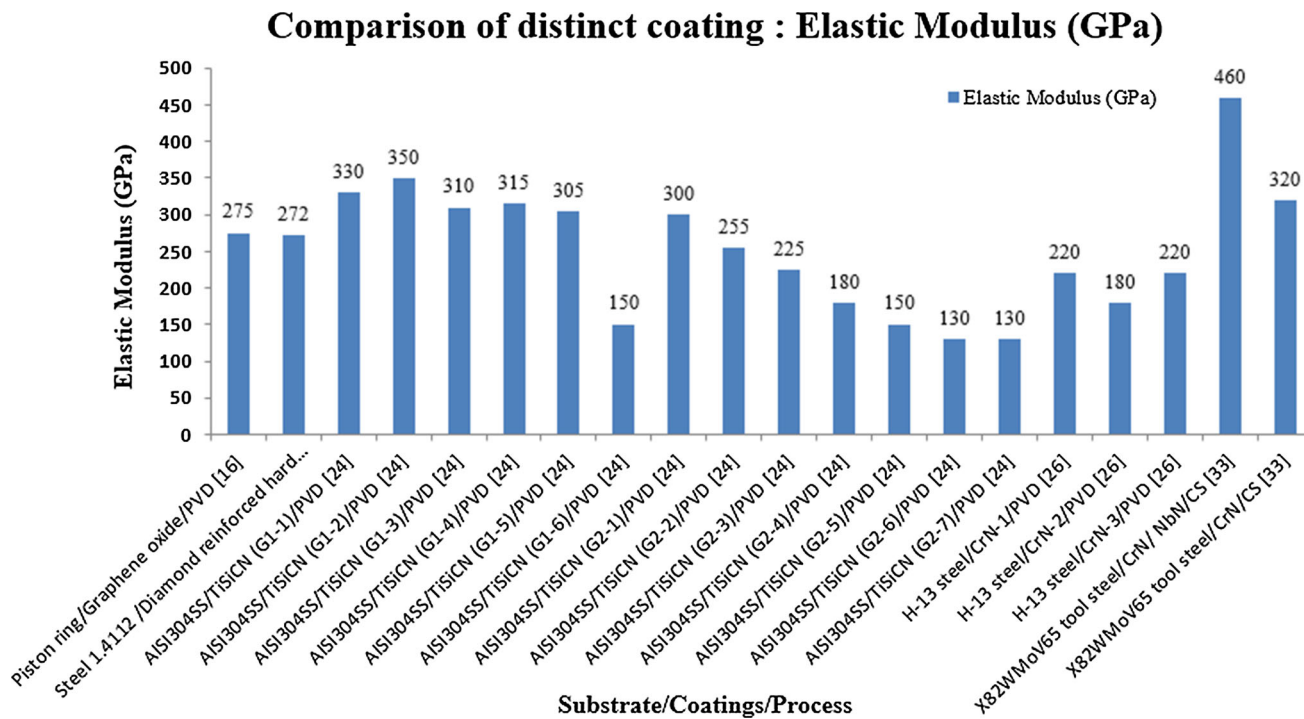


Fig. 14 Coating elastic modulus (GPa) Vs. substrate/coating/process by distinct processes on piston/cylinder liner materials

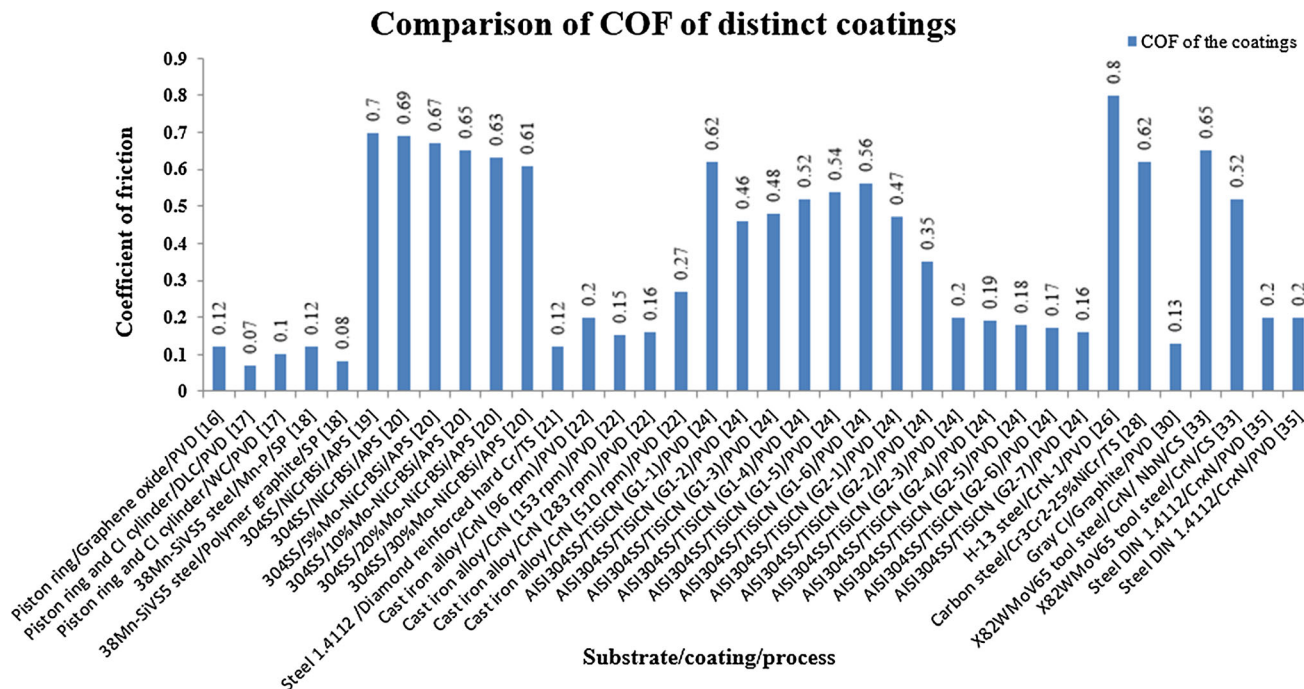


Fig. 15 Coefficient of friction (COF) of distinct coating Vs. substrate/coating/process by distinct processes on piston/cylinder liner materials

Design Modification

By improving the design of bowl rim and pin bore, failure of the piston can be reduced. By increasing the diameter and reducing the depth of the bowl, piston strength can be

improved [57–59]. Thus, there is a need to modify the design that enhances the strength of pin bore and reduces the bowl stresses. Thus, the life of the piston can be increased.

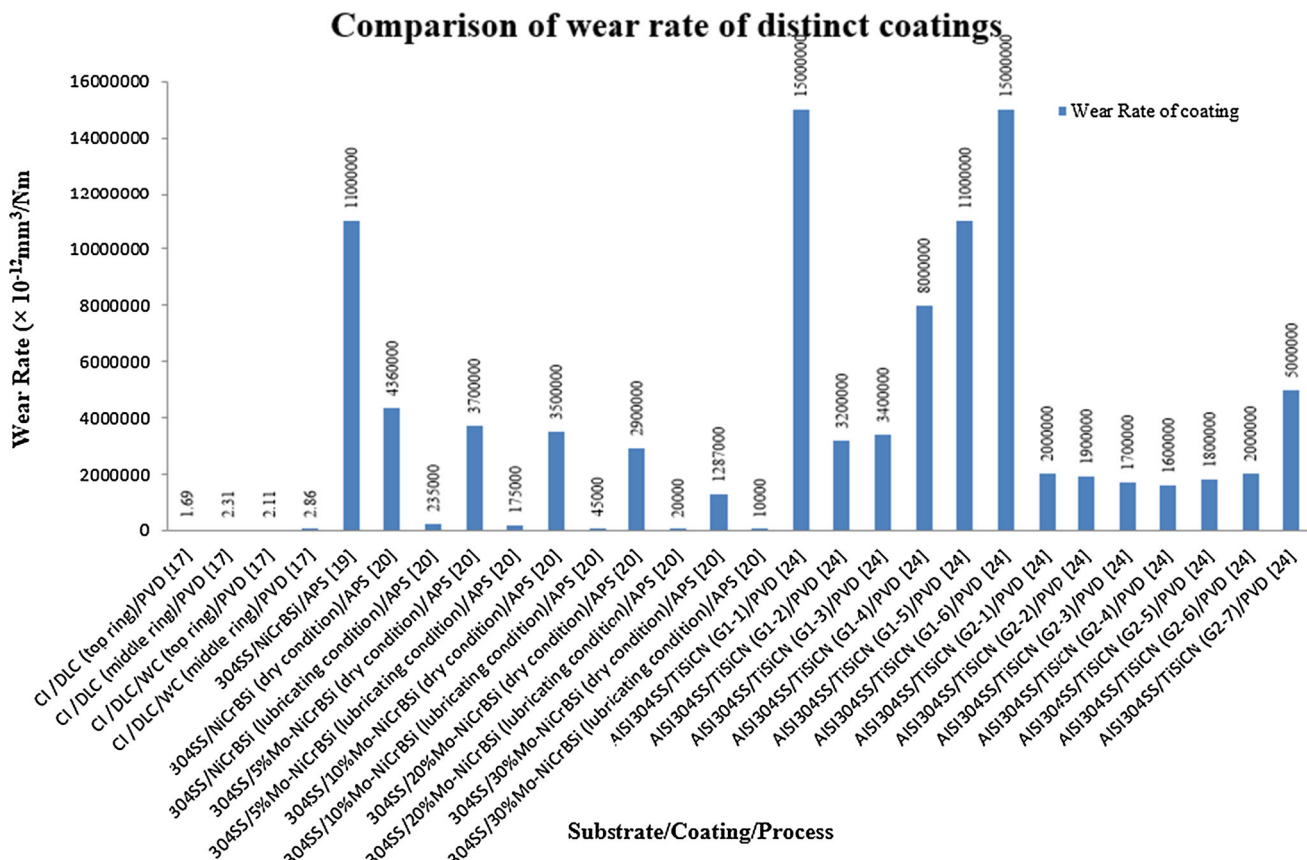


Fig. 16 Wear rate of distinct coating Vs. substrate/coating/process by distinct processes on piston/cylinder liner materials

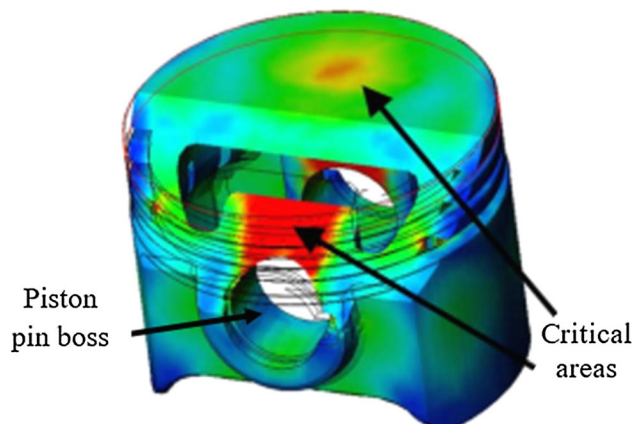


Fig. 17 Piston failure due to stress concentration near pinhole. Reprinted by permission from Elsevier: Elsevier, *Engineering Failure Analysis*, Fatigue on engine pistons—A compendium of case studies, F.S. Silva, Copyright 2006, [37]

By using Inserts or Shrink Fitted Parts

The use of alumina fiber inserts is used to enhance the properties of components. It can be used in pin bore area and bowl rim in the piston crown [60].

Piston Cooling

The maximum temperature of the piston can be reduced by flowing the oil through a cooling channel or by an oil spray jet directed at the bottom of the piston. This will be useful to prevent the premature failure of the piston [37].

Summary

Mechanical friction is one of the primary types of energy loss in an internal combustion engine. Mishra et al. [61] reported the distinct sources that are contributing the whole losses in an IC engine as shown in Fig. 20.

However, the failure of the piston system in IC engine is a common problem. The results of previous investigations revealed that 15% of entire input fuel energy in an internal combustion engine is lost owing to the friction/wear of various moving parts. However, a slight modification in the geometry or surface of the part can save money.

As the piston compression ring is positioned on the top of the piston assembly and accounts for about eight percent of the piston subsystem loss. This loss may be owing to the mechanical friction developed because of the concurrent

Combustion area

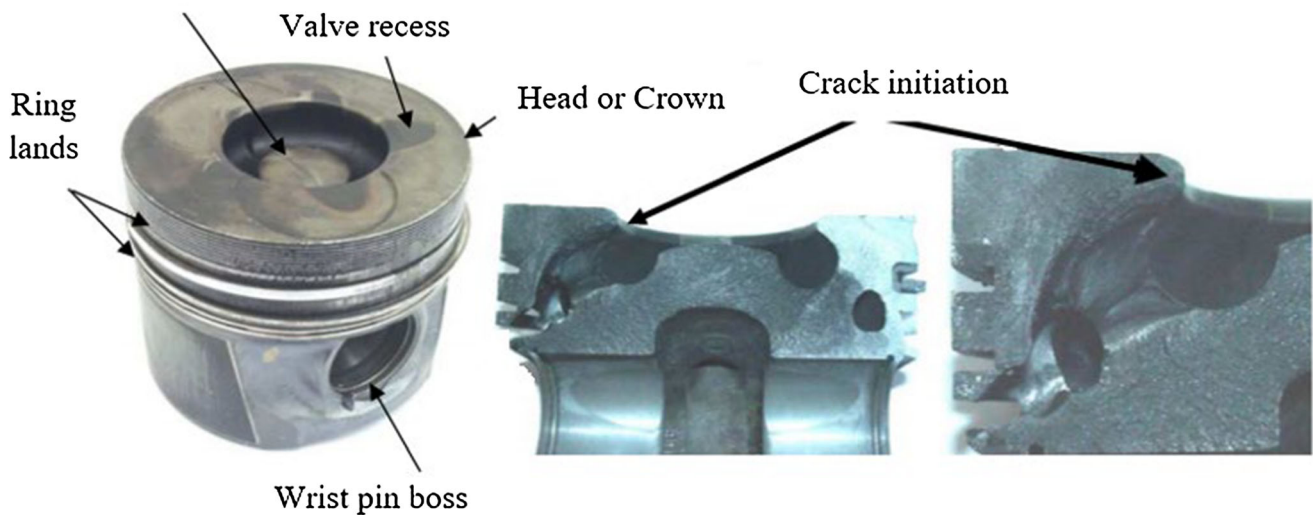


Fig. 18 Compression ignition engine piston with cooling gallery showing a crack from one side of the pinhole to the head. Reprinted by permission from Elsevier: Elsevier, *Engineering Failure Analysis*,

Fatigue on engine pistons—A compendium of case studies, F.S. Silva, Copyright 2006, [37]

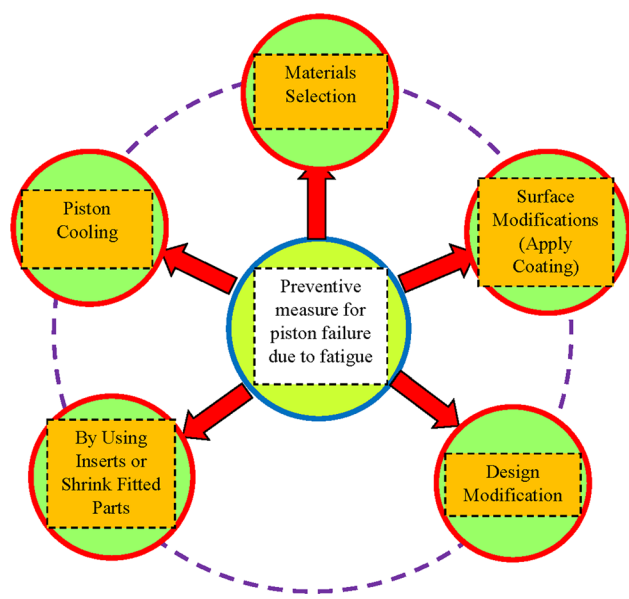


Fig. 19 Preventive measures for piston failure due to fatigue [37]

sliding action and sealing. However, these losses can be reduced by improving the design of piston ring and its manufacturing techniques [62, 63]. According to Kulkarni et al [64] the failure of the piston can be due to many reasons such as improper maintenance, improper failure of lubrication system, improper fuel injection timing, manufacturing defects, high wear and friction during operation, etc. But, most of the time, the failure of piston can be detected by early diagnosis. These diagnoses include loss of cooling water, change in peak firing pressure and knocking tendency in cylinder, etc. Thus, proper

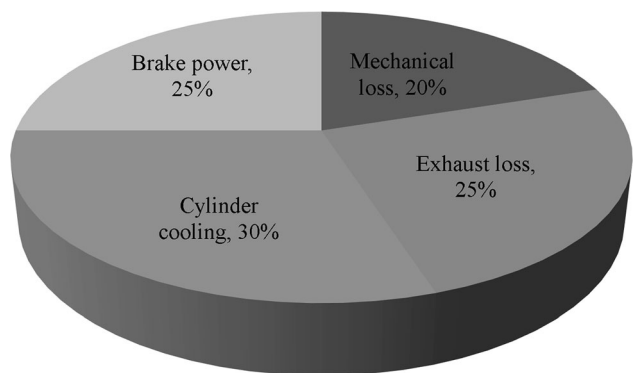


Fig. 20 Share of distinct losses in an IC engine [61]

maintenance and checking are required to prevent premature failure of the piston.

Conclusions

This paper provides an overview of possible causes of piston failure and their preventive measures. Among distinct preventive measures, coating is an effective approach to reduce piston failures. Further, the distinct coatings deposited on piston and piston rings using distinct thermal spray processes to evaluate their performance in terms of friction and wear losses are summarized. Then, based upon literature survey following conclusions were made:

- (1) The hard coatings, such as chromium compounds and compounds of other transition metals (as Ti)

- deposited by physical vapor deposition techniques provide better results in case of compression ring.
- (2) CrN coatings offered excellent tribological performance in case of top piston rings.
 - (3) For piston ring, low-pressure plasma-sprayed ceramic, metal composite coating offered better wear-resistant properties. In addition, HVOF sprayed CrC–NiCr can be used in place of hard Cr coating depending upon various factors such as COF, cost and environmental issues.
 - (4) From the literature, it is clear that H-13 steel coated with CrN material using physical vapor deposition methods produces least roughness, while Gray cast iron coated with graphite and diamond-like carbon (DLC) produces maximum roughness.
 - (5) NbN/CrN nanoscale multilayer coating deposited on AISI4408 piston ring using PVD provides maximum hardness
 - (6) AISI304SS coated with TiSiCN using a PVD process gives the least elastic modulus (GPa), while the X82WMoV65 tool steel coated with CrN/NbN material by using a cathode switching reactive cathodic arc evaporative method gives maximum elastic modulus value.
 - (7) Piston ring and CI cylinder coated with diamond-like carbon (DLC) using physical vapor deposition process have least COF, while H-13 steel coated with CrN-1 material using PVD process have maximum COF.
 - (8) Cast iron coated with diamond-like carbon using PVD offered least wear rate, while the TiSiCN coating deposited on AISI304SS material offered maximum wear rate, although less literature is available on diamond-like carbon coatings and need to explore.

Future Scope and Challenges

Post-heat treatment of as-sprayed coatings can be done to attain a dense coating having high adhesion and cohesion strengths. Liu et al. [19] also used the post-heat treatment on plasma-sprayed NiCrBSi coatings at three distinct temperatures (300, 500 and 700 °C). The results revealed that with the increase in heat treatment temperature, the crystallinity of the as-sprayed coating was significantly increased. Further, heat treatment enhances the micro-hardness of the coating, whereas it did not exert a prominent influence on the friction coefficients of the as-sprayed coatings. However, more research is required to study the effect of post-coating heat treatment parameters and methods on the microstructure, micro-hardness, phase

composition, wear rate, friction, and corrosion performance of the coating. In addition, there exists a theoretical gap in technology of the seizure physics and therefore advanced theories should be developed in the future to improve the understanding of this complex seizure mechanism.

Acknowledgment Authors are highly thankful to R&D Department of Chandigarh Group of College Landran, Mohali, Punjab, for their support and contribution.

References

1. J.L. González, D. Rivas, M.A. Beltrán, Failure Analysis of a Diesel Engine. *Procedia Struct. Integr.* **3**, 41–47 (2017). <https://doi.org/10.1016/j.prostr.2017.04.007>
2. V.R. Deulgaonkar, N. Ingolikar, A. Borkar, S. Ghute, N. Awate, Failure Analysis of Diesel Engine Piston in Transport Utility Vehicles. *Eng. Fail. Anal.* **120**, 105008 (2021). <https://doi.org/10.1016/j.engfailanal.2020.105008>
3. Q.M. Mehran, M.A. Fazal, A.R. Bushroa, S. Rubaiee, A Critical Review on Physical Vapor Deposition Coatings Applied on Different Engine Components. *Crit. Rev. Solid State Mater. Sci.* (2017). <https://doi.org/10.1080/10408436.2017.1320648>
4. J.B. Heywood, *Internal Combustion Engine Fundamentals*. (McGraw Hill, 1988)
5. M. Hoshi, Reducing Friction Losses in Automobile Engines. *Tribol. Int.* **17**(4), 185–189 (1984). [https://doi.org/10.1016/0301-679X\(84\)90017-3](https://doi.org/10.1016/0301-679X(84)90017-3)
6. Y. Enomoto, T. Yamamoto, New Materials in Automotive Tribology. *Tribol. Lett.* **5**, 13–24 (1998). <https://doi.org/10.1023/A:1019100531912>
7. G. Offner, N. Lorenz, O. Knaus, Piston Clearance Optimization using Thermo-Elasto Hydrodynamic Simulation to Reduce Piston Slap Excitation and Friction Loss. *SAE Tech. Pap.* 2012-01-1530. (2012). <https://doi.org/10.4271/2012-01-1530>
8. K. Nakayama, Y. Yasutake, M. Takiguti, S. Furuhama, Effect of Piston Motion on Piston Skirt Friction of a Gasoline Engine. *SAE Tech. Pap.* 970839. (1997). <https://doi.org/10.4271/970839>
9. M. Takiguchi, H. Kikuchi, S. Furuhama, Influence of Clearance Between Piston and Cylinder on Piston Friction. *SAE Tech. Pap.* 881621. (1988). <https://doi.org/10.4271/881621>
10. O.P. Singh, Y. Umbarkar, T. Sreenivasulu, E. Vettrivendan, M. Kannan, Y.R. Babu, Piston Seizure Investigation: Experiments, Modeling and Future Challenges. *Eng. Fail. Anal.* **28**, 302–310 (2013). <https://doi.org/10.1016/j.engfailanal.2012.11.005>
11. M. J. Neale, B14 - Piston and Ring Failures, Lubrication and Reliability Handbook, Butterworth-Heinemann, 2001, pp 1-5. <https://doi.org/10.1016/B978-075065154-7/50108-X>
12. K. Nakayama, Y. Yasutake, M. Takiguti, S. Furuhama, Effect of Piston Motion on Piston Skirt Friction of a Gasoline Engine 970839. *SAE Tech. Pap.* (1997). <https://doi.org/10.4271/970839>
13. K. Bewilogua, G. Bräuer, A. Dietz, J. Gfäbler, G. Goch, B. Karpuschewski, B. Szyszka, Surface Technology for Automotive Engineering. *CIRP Ann. Manufact. Technol.* **58**(2), 608–627 (2009)
14. R. Niculescu, V. Lorga-Siman, A. Trica et al., Study on the Engine oil's Wear based on the Flash Point. *Mater Sci Eng.* **47**, 1–9 (2016). <https://doi.org/10.1088/1757-899X/147/1/012124>
15. S. Tung and Y. Cheng, Tribological Characteristics and Microstructures of PVD thin film Coatings on Steel Substrates, Proc. International Wear Conference, San Francisco, CA, 1993.
16. D. Özkan, Y. Erarslan, C. Kincal, O. Gürlü, M.B. Yağcı, Wear and Corrosion Resistance Enhancement of Chromium Surfaces

- Through Graphene Oxide Coating. *Surf. Coat. Technol.* **391**(125595), 1–10 (2020). <https://doi.org/10.1016/j.surfcoat.2020.125595>
- 17. V. Kumar, S.K. Sinha, A.K. Agarwal, Wear Evaluation of Engine Piston Rings Coated With Dual Layer Hard and Soft Coatings. *J. Tribol.* **141**(3), 1–24 (2018). <https://doi.org/10.1115/1.4041762>
 - 18. A.H. Shaw, J. Qu, C. Wang, R.D. England, Tribological Study of Diesel Piston Skirt Coatings in CJ-4 and PC-11 Engine Oils. *Wear.* **376–377**, 1673–1681 (2017). <https://doi.org/10.1016/j.wear.2017.01.082>
 - 19. L. Liu, H. Xu, J. Xiao, X. Wei, G. Zhang, C. Zhang, Effect of Heat Treatment on Structure and Property Evolutions of Atmospheric Plasma Sprayed NiCrBSi Coatings. *Surf. Coat. Technol.* **325**, 548–554 (2017). <https://doi.org/10.1016/j.surfcoat.2017.07.011>
 - 20. C. Zhang, L. Liu, H. Xu, J. Xiao, G. Zhang, H. Liao, Role of Mo on Tribological Properties of Atmospheric Plasma-sprayed Mo-NiCrBSi Composite Coatings under Dry and Oil-lubricated Conditions. *J. Alloy. Compd.* **727**, 841–850 (2017). <https://doi.org/10.1016/j.jallcom.2017.08.195>
 - 21. J. Biberger, H.J. Füßer, Development of a Test Method for a Realistic, Single Parameter-dependent Analysis of Piston Ring versus Cylinder Liner Contacts with a Rotational Tribometer. *Tribol. Int.* **113**, 111–124 (2017). <https://doi.org/10.1016/j.triboint.2016.10.043>
 - 22. S. K. Singh, S. Chattopadhyaya, A. Pramanik, S. Kumar, Wear Behavior of Chromium Nitride Coating in Dry Condition at Lower Sliding Velocity and Load, *Int. J. Adv. Manuf. Technol.*, 2017, 1–11, p 1665–1675. <https://link.springer.com/article/10.1007%2Fs00170-017-0796-x>
 - 23. S. Pal, A. Deore, A. Choudhary, V. Madhwani, D. Vijapuri, Analysis and Experimental Investigation of Ceramic Powder Coating on Aluminium Piston. *IOP Conf. Ser.: Mater. Sci. Eng.* **263**, 062071 (2017). <https://doi.org/10.1088/1757-899X/263/6/062071>
 - 24. J. Lin, R. Wei, D.C. Bitsis, P.M. Lee, Development and Evaluation of Low Friction TiSiCNanocomposite Coatings for Piston Ring Applications. *Surf. Coatings Technol.* **298**, 121–131 (2016). <https://doi.org/10.1016/j.surfcoat.2016.04.061>
 - 25. J.A. Araujo, G.M. Araujo, R.M. Souza, A.P. Tschiptschin, Effect of Periodicity on Hardness and Scratch Resistance of CrN/NbNNanoscale Multilayer Coating Deposited by Cathodic Arc Technique. *Wear.* **330–331**, 469–477 (2015). <https://doi.org/10.1016/j.wear.2015.01.051>
 - 26. C.L. Martin, O.O. Ajayi, S. Torrel, N. Demas, A. Erdemir, R. Wei, Effect of Coating Thickness on Tribological Performance of CrN in Dry Sliding Contact, ASME, STLE. *Int. Jt. Tribol. Conf.* Denver Colorado, USA. **2012**, 10–12 (2012)
 - 27. A. Igartua, X.F. Perez, M. Conte, and I. Illarramendi, Tribological Test to Simulate Wear on Piston Ring, In: Proceeding of the 24th International Congress on Condition Monitoring and Diagnostics Engineering Management, 2011, p 1–10.
 - 28. S. Houdková, M. Kašparová, F. Zahálka, The Friction Properties of the HVOF Sprayed Coatings Suitable for Combustion Engines, Measured in Compliance with ASTM G-99, *WIT Trans. Eng. Sci.* **66**, 129–139 (2010)
 - 29. J.H. Jang, B.D. Joo, J.H. Lee, Y.H. Moon, Effect of Hardness of the Piston ring Coating on Wear Characteristics of Rubbing Surfaces. *Met. Mater. Int.* **15**(6), 903–908 (2009)
 - 30. D.H. Cho, S.A. Lee, Y.Z. Lee, The Effects of Surface Roughness and Coatings on the Tribological Behavior of the Surfaces of a Piston Skirt. *Tribol. Trans.* **53**(1), 137–144 (2009). <https://doi.org/10.1080/10402000903283276>
 - 31. A. Skopp, N. Kelling, M. Woydt, L.M. Berger, Thermally Sprayed Titanium Suboxide Coatings for Piston Ring/Cylinder Liners under Mixed Lubrication and Dry-Running Conditions. *Wear.* **262**(9–10), 1061–1070 (2007). <https://doi.org/10.1016/j.wear.2006.11.012>
 - 32. M.B. Karamış, K. Yıldızlı, H. Çakırer, An Evaluation of Surface Properties and Frictional Forces Generated from Al-Mo-Ni Coating on Piston Ring. *Appl. Surf. Sci.* **230**, 191–200 (2004). <https://doi.org/10.1016/j.apsusc.2004.02.053>
 - 33. E. Bemporad, C. Pecchio, S. De Rossi, F. Carassiti, Characterisation and Wear Properties of Industrially Produced Nanoscaled CrN/NbN Multilayer Coating. *Surf. Coat. Technol.* **188–189**, 319–330 (2004). <https://doi.org/10.1016/J.Surfcoat.2004.08.069>
 - 34. S. Zhuo, Z. Peijun, Z. Leheng, X. Xinfu, H. Aimin, Z. Wenquan, Multi-layer Compound Coating on Cast Iron Piston Ring by Multi-arc and Magnetron Sputtering Ion Compound Plating Technique. *Surf. Coat. Technol.* **131**, 422–427 (2000). [https://doi.org/10.1016/S0257-8972\(00\)00781-7](https://doi.org/10.1016/S0257-8972(00)00781-7)
 - 35. C. Friedrich, G. Berg, E. Broszeit, F. Rick, J. Holland, PVD CrxN Coatings for Tribological Application on Piston Rings. *Surf. Coat. Technol.* **97**(1–3), 661–668 (1997). [https://doi.org/10.1016/s0257-8972\(97\)00335-6](https://doi.org/10.1016/s0257-8972(97)00335-6)
 - 36. P.M. Patel, N.R. Makwana, N.A. Patel, P.D. Patel, Recent Trends To Increase The Service Life Of The Engine With The Help Of Improvement Of Wear Resistance Of Piston Ring – A. Rev. Stud. **2**(4), 1984–1992 (2013)
 - 37. F.S. Silva, Fatigue on Engine Pistons – A compendium of Case Studies. *Eng. Fail. Anal.* **13**(3), 480–492 (2006). <https://doi.org/10.1016/j.engfailanal.2004.12.023>
 - 38. D. Liu, D.J. Pons, Crack Propagation Mechanisms for Creep Fatigue: A Consolidated Explanation of Fundamental Behaviours from Initiation to Failure. *Metals.* **8**, 1–32 (2018)
 - 39. G. Floweday, S. Petrov, R.B. Tait, Thermo-Mechanical Fatigue Damage and Failure of Modern High Performance Diesel Pistons. *J. Press.* **18**(7), 1664–1674 (2011). <https://doi.org/10.1016/j.engfailanal.2011.02.002>
 - 40. S. Reichstein, P. Konrad, S. Kenningly, F.T.H. Doernenburg, Microstructure Modification–Piston Materials for High Stress and Temperature Conditions. *ATZ Autotechnol.* **8**(6), 42–47 (2008)
 - 41. H.L. Ewalds, R.J.H. Wanhill, Fatigue crack growth, in *Fracture mechanics*. (Edward Arnold, London, 1984), p 207–44
 - 42. Reichstein S, Weis R, Kenningly S, Lades K, Konrad P, Doernenburg FTH. High-performance cast aluminum pistons for highly efficient diesel engines, in 2007 SAE World Congress, SAE 2007-01-1438; 2007.
 - 43. C. Li, Piston Thermal Deformation and Friction Considerations. *SAE Tech. Pap.* 820086. (1982). <https://doi.org/10.4271/820086>
 - 44. M. Takiguchi, H. Kikuchi, S. Furuhama, Influence of clearance between piston and cylinder on piston friction. *SAE Tech. Pap.* 881621. (1988). <https://doi.org/10.4271/881621>
 - 45. M.R. Joyce, C.M. Styles, P.A.S. Reed, Elevated Temperature Short Crack Fatigue behavior In Near Eutectic Al-Si alloys. *Int. J. Fatigue.* **25**, 863–869 (2003). [https://doi.org/10.1016/S0142-1123\(03\)00157-9](https://doi.org/10.1016/S0142-1123(03)00157-9)
 - 46. K. Nakajima, H. Otaka, T. Kashimura, S. Sakuma, M. Tanaka, Newly Developed Hollow Ring Groove Insert Piston-Part 2: Producing Technology of New Piston. *JSAE Rev.* **17**(4), 448 (1996)
 - 47. F. Payri, J. Benajes, X. Margot, A. Gil, CFD Modeling of the In-cylinder Flow in Direct-Injection Diesel Engines. *Comput. Fluids.* **33**(8), 995–1021 (2004)
 - 48. R. Mogilewski, S.R. Brian, W.S. Wolbach, T.W. Krusek, R.D. Maier, D.L. Shoemaker, J.M. Chabala, K.K. Soni, R. Levi-Setti, Reactions at the Matrix-Reinforcement Interface in Aluminum Alloy Matrix Composites. *Mater. Sci. Eng. A.* **191**, 209–222 (1995)

49. Y.D. Huang, N. Hort, K.U. Kainer, Thermal Behavior of Short Fiber Reinforced AlSi12CuMgNi Piston Alloys. *Compos. A.* **35**(2), 249–263 (2004)
50. M. Vijaya Babu, R. Krishna Kumar, O. Prabhakar, S.N. Gowri, Fracture Mechanics Approaches to Coating Strength Evaluation. *Eng. Fract. Mech.* **55**(2), 235–248 (1996)
51. K. Nakajima, H. Otaka, T. Kashimura, S. Sakuma, M. Tanaka, Newly Developed Hollow Ring Groove Insert Piston—part 2: Producing Technology of New Piston. *JSAE Rev.* **17**(4), 448 (1996)
52. S. Kumar, M. Kumar, A. Handa, Erosion Corrosion Behavior and Mechanical Property of Wire Arc Sprayed Ni-Cr and Ni-Al Coating on Boiler Steels in Actual Boiler Environment. *Mater. High Temp.* **37**(6), 1–15 (2020). <https://doi.org/10.1080/09603409.2020.1810922>
53. S. Kumar, M. Kumar, A. Handa, Comparative Study of High Temperature Oxidation Behavior of Wire Arc Sprayed Ni-Cr And Ni-Al Coatings. *Eng. Fail. Anal.* **106**, 104173–104189 (2019)
54. S. Kumar, M. Kumar, A. Handa, Combating Hot Corrosion of Boiler Tubes- A Study. *J. Eng. Fail. Anal.* **94**, 379–395 (2018). <https://doi.org/10.1016/j.englfailanal.2018.08.004>
55. R. Kumar, S. Kumar, Thermal Spray Coating Process: A Study. *Int. J. Eng. Sci. Res. Technol.* **7**(3), 610–617 (2018)
56. S. Kumar, R. Kumar, S. Singh, H. Singh, A. Handa, The Role of Thermal Spray Coating to Combat Hot Corrosion of Boiler Tubes: A Study. *J. Xidian Univ.* **14**(5), 229–239 (2020). <https://doi.org/10.37896/jxu14.5/024>
57. P.C. Miles, Ing. Ö. Andersson. A review of design considerations for light-duty diesel combustion systems. *Sitzung*, pp. 1–15. <https://www.osti.gov/servlets/purl/1240837>.
58. M.J. Valco, Spherical Joint Piston and Connecting Rod Developed. *NASA Rep.* **216**, 433–3717 (2000)
59. B.C. Kaul, E.J. Nafziger, M.D. Kass, Enterprise: a reduced-scale, flexible fuel, single-cylinder crosshead marine diesel research engine, CIMAC Congress 2019, Vancouver, pp. 1–19.
60. Z. Pan, L. Guo, Failure Analysis of the Pin Bore of the Combined Piston for the Aero Engine. *Int. J. Aerosp. Eng.* **2019**(7693403), 1–13 (2019). <https://doi.org/10.1155/2019/7693403>
61. P.C. Mishra, A Review of Piston Compression Ring Tribology. *Tribol. Ind.* **36**(3), 269–280 (2014)
62. R. Rahmani, S. Theodossiades, H. Rahnejat, B. Fitzsimons, Transient Elastohydrodynamic Lubrication of Rough New or Worn Piston Compression Ring Conjunction with an Out-of-round Cylinder Bore. *Proc. IMechE, Part J: J. Eng. Tribol.* **226**(4), 284–305 (2012)
63. P.C. Mishra, Tribodynamic Modeling of Piston Compression Ring Cylinder Liner Contact at High Pressure Zone of Engine Cycle. *Int. J. Adv. Manuf. Technol.* **66**(5–8), 1075–1085 (2013)
64. N. Kulkarni, G. Chaware, Analysis of Piston Failure: A Review. *IJIET.* **6**(3), 138–146 (2016)

Publisher's Note Springer Nature remains neutral with regard to jurisdictional claims in published maps and institutional affiliations.